Comprehensive Summaries of Uppsala Dissertations
from the Faculty of Science and Technology 714

Studies of Nuclear Fuel by Means of Nuclear Spectroscopic Methods

BY

PETER JANSSON

ACTA UNIVERSITATIS UPSALIENSIS
UPPSALA 2002

Dissertation for the Degree of Doctor of Philosophy in Nuclear Physics presented at Uppsala University in 2002.

ABSTRACT
Jansson, P. 2002. Studies of Nuclear Fuel by Means of Nuclear Spectroscopic Methods. Acta Universitatis Upsaliensis. *Comprehensive Summaries of Uppsala Dissertations from the Faculty of Science and Technology* 714. 81 pp. Uppsala. ISBN 91-554-5315-5.

The increasing demand for characterization of nuclear fuel, both from an operator and authority point of view, motivates the development of new experimental and, preferable, non-destructive methods. In this thesis, some methods based on nuclear spectroscopic techniques are presented.

Various parameters of irradiated fuel are shown to be determined with high accuracy and confidence by utilizing gamma-ray scanning, tomography and passive neutron assay.

Specifically, fuel parameters relevant for a secure storage of spent nuclear fuel in a long-term repository, such as e.g. burnup and decay heat, are shown to be determined with adequate accuracy. The techniques developed are expected to be implemented in the planned encapsulation facility in Sweden.

Also, a device for tomographic measurements of the spatial distribution of thermal power in nuclear fuel assemblies has been built, tested and evaluated. The device utilizes single photon emission computed tomography (SPECT) in order to reconstruct the gamma-ray source distribution within a fuel assembly. The device is expected to be an important tool for validating reactor core simulators regarding new fuel designs.

For safeguards purposes, two experimental methods for verifying the integrity, i.e. the possible loss of fissile material from a nuclear fuel assembly, are presented. Verification of integrity is shown to be possible on an individual fuel rod level.

Peter Jansson, Department of Radiation Sciences,
Uppsala University, Box 535, SE-75121, Uppsala, Sweden

ISSN 1104-232X
ISBN 91-554-5315-5

Printed in Sweden by Fyris Tryck AB, Uppsala 2002.
Distributor: Uppsala University Library, Uppsala, Sweden.

Till min mor, syster, far och Sonny.

Contents

List of Tables

List of Figures

Chapter 1

Introduction

1.1 The nuclear reactor

On December 2, 1942, Enrico Fermi demonstrated the first working nuclear reactor in the football stadium at the University of Chicago, USA, see e.g. ref. [1]. The construction of the first reactor followed after some years of intense research and development, initially based on military reasons but, eventually, with focus on developing nuclear power for civilian use and generation of electric power.

As of December 31, 2000, 438 nuclear power reactors are in operation worldwide. These reactors supplied about 2450 TWh of electric energy to the power grid during the year 2000. Furthermore, during the same year, 31 power reactors were under construction. In total, 9820 years of operating experience were established until the end of year 2000, see ref. [2].

1.1.1 Basic principles

The nuclear power reactor is based on the principle of a neutron induced, sustained, fission chain reaction. Nuclear fission is the process in which a nucleus breaks into two or more fission fragments. Besides the fission fragments, beta and neutrino particles, prompt gamma-rays and neutrons are emitted. The chain reaction is made possible by the fission neutrons, i.e., in each fission, more than one neutron is produced which, in principle, enables additional fissions. In the fission of one ^{235}U nucleus, about 200 MeV of energy is produced. The fission fragments acquire about 80 % of this energy, the remaining energy being distributed among the other particles and emitted as radiation.

It is a well-known feature of the binding energy per nucleon that it exhibits a maximum energy of about 9 MeV in a region around A = 60, see e.g. refs. [1,

3]. This fact implies that energy, in principle, is released when two light nuclei are fused together while for heavier nuclei, energy is released when nuclei are fissioning. From this arguing one would expect all nuclei heavier than about A = 100 to fission. The fact that such nuclei are observed in nature is due to a subtle interplay between the Coulomb- and the nuclear forces acting within a nucleus that prevent such nuclei to fission spontaneously. However, some nuclei indeed fission spontaneously, which is due to the zero-point energy of the nuclear motions which, through the quantum mechanical effect of tunneling, causes a small probability of fission even below the activation energy.

For some nuclei, so called *fissile* nuclei, e.g. ^{233}U, ^{235}U and ^{239}Pu, capture of a thermal neutron results in a compound nucleus that fissions. For yet some other nuclei, e.g. ^{232}Th and ^{238}U, fission is made possible by capture of a fast neutron. The latter ones may also be transformed into fissile isotopes by neutron capture reactions.

The two fission fragments produced in fission of ^{235}U by thermal neutrons are usually of unequal mass, with the lighter fragment in the range of mass numbers 80-110 and the heavier mass in the range 125-150. Two maxima in the fission fragment mass distribution are observed at mass numbers A$\approx$95 and A$\approx$140, respectively. For thermal fission of ^{235}U, the fission fragment mass yield curve is shown in figure 1.1. The mass distribution of the fission fragments is a function of the energy of the captured neutron; the asymmetry observed for thermal neutrons disappears at higher neutron energies. For 90 MeV neutrons, a symmetric distribution of the fission fragments has been observed [1].

Two neutron production mechanisms can usually be observed in conjunction with fission: Prompt neutrons emitted during the fission process and delayed neutrons emitted from the decay of neutron-rich fission fragments. The energy distribution of the prompt neutrons range from very low energies up to about 10 MeV, usually the distribution is described by either a Maxwellian $f(E) \sim \sqrt{E/T^3} \cdot \exp(-E/T)$ or by a semi-empirical expression of the form $f(E) \sim C \cdot \exp(-E/a) \cdot \sinh\left(\sqrt{bE}\right)$. The mean energy of the prompt neutrons is about 2 MeV. The mean energy of the delayed neutrons is about 0.4 MeV [1, 3]. In technical applications, the delayed neutrons are usually divided into six groups where each group has a well-defined half life of the delayed neutron precursors. The half life of these groups range from 0.2 s up to 54 s.

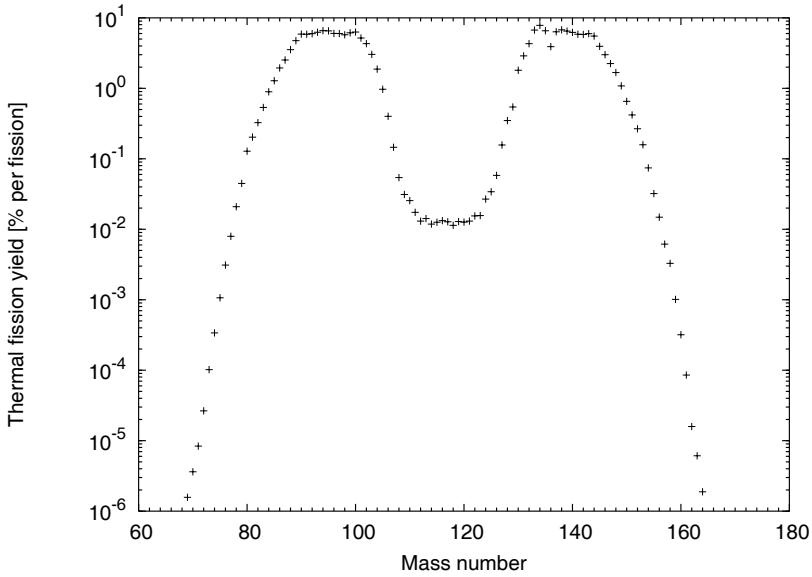

Figure 1.1: *The distribution of fission fragment mass from thermal fission of* ^{235}U*. Based on data from [4] as reported by [5].*

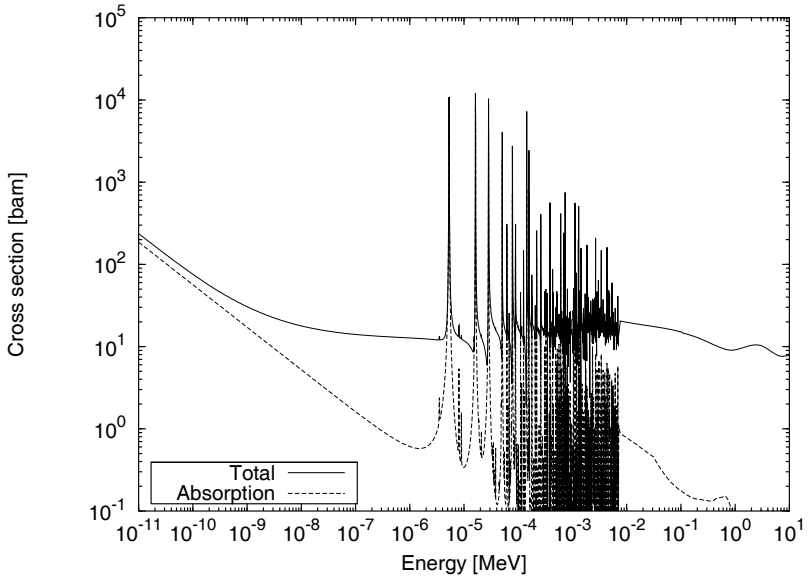

Figure 1.2: *Neutron reaction cross-sections for* ^{238}U*. Data from [6].*

1.1.2 Technical principles

In order to obtain a chain reaction, the fast neutrons produced in fission must be slowed down, "moderated", into the region of thermal energy, where the fission cross-section for ^{235}U is large. This can be achieved by scattering processes in various material. It is important that this moderation procedure is rapid since the neutrons, in their passage from higher energies to low energy, have to pass through the region of strong neutron capture resonances in ^{238}U, cf. figure 1.2. For this the uranium fuel has to be combined with a moderator that provides a large energy loss in the scattering process.

Denoting the average logarithmic energy decrement in elastic scattering by ξ, defined in equation 1.1, one may form a quantity $\xi\Sigma_s/\Sigma_a$ that represents a "figure of merit" of a moderator; i.e., the higher the value of this quantity, the better is the moderator in thermalizing the neutrons. Here, $\Sigma_{a,s}$ are the macroscopic absorption and scattering cross-sections, respectively. Table 1.1 shows values of this quantity for some materials. As may be seen from table 1.1, efficient moderators are D_2O, C, Be, ^{4}He or H_2O.

$$\xi = \overline{\ln\left(\frac{E}{E'}\right)} = 1 + \frac{(A-1)^2}{2A} \cdot \ln\left(\frac{A-1}{A+1}\right) \tag{1.1}$$

Material	A	ξ	$\xi\Sigma_s/\Sigma_a$
^{1}H	1	1.0	
^{2}D	2	0.726	
^{4}He	4	0.425	83
^{6}Li	6	0.299	0.0059
^{9}Be	9	0.207	143
^{10}B	10	0.187	0.00062
^{12}C	12	0.158	192
^{238}U	238	0.0084	0.009
H_2O		0.920	71
D_2O		0.509	5670

Table 1.1: *Characteristic parameters of some materials that may be used as moderators in a nuclear reactor. Data from [1].*

The basis for the design, control and operation of a nuclear reactor is the distribution of the neutron flux density within the nuclear reactor. The transport of neutrons can be described by the Boltzmann transport equation 1.2, which can be solved to yield the neutron flux density ϕ as a function of position $\vec{r}$, direction $\vec{\Omega}$, energy E and time t. The transport equation states

the neutron conservation in an infinitesimal volume-energy-angle element. It is a linear equation since neutron-neutron collisions are assumed insignificant.

$$\begin{aligned}
&\left[\tfrac{1}{v}\tfrac{\partial}{\partial t} + \vec{\Omega}\cdot\vec{\nabla} + \Sigma\left(\vec{r},E,t\right)\right]\phi\left(\vec{r},\vec{\Omega},E,t\right) \\
&\quad = \int_0^\infty \int_{4\pi} \phi\left(\vec{r},\vec{\Omega}',E',t\right)\Sigma_s\left(\vec{r},\vec{\Omega}'\to\vec{\Omega},E'\to E,t\right)d\vec{\Omega}'dE' \\
&\quad + \tfrac{\chi_p(E)}{4\pi}\int_0^\infty \int_{4\pi} (1-\beta)\,\nu\left(\vec{r},E'\right)\phi\left(\vec{r},\vec{\Omega}',E',t\right)\Sigma_f\left(\vec{r},E',t\right)d\vec{\Omega}'dE' \\
&\quad + \tfrac{1}{4\pi}\sum_j \chi_j\left(E\right)\lambda_j C_j\left(\vec{r},t\right) + S\left(\vec{r},\vec{\Omega},E,t\right)
\end{aligned} \tag{1.2}$$

Here,

- ϕ is the neutron flux density,
- Σ_s is the double differential cross-section, i.e. the probability that a neutron is scattered into the element $dVd\vec{\Omega}dE$,
- χ_p is the energy distribution of prompt neutrons, normalized to unity,
- $\beta = \sum_j \beta_j$, where β_j is the fraction of neutrons born in fission that arise from decay of the j^{th} group of precursors,
- ν is the average number of neutrons born in fission,
- Σ_f is the double differential fission cross-section,
- C_j is the average density of precursors in the j^{th} group with the corresponding decay constant λ_j and energy spectrum χ_j,
- S is the angular source density of independent neutron sources.

The fission reaction results in production of neutrons that may induce further fissions in a chain reaction. Control of the reactor is based on controlling the fission chain reaction. Denoting the multiplication of the number of neutrons generated in the chain reaction by k, see equation 1.3, the chain reaction is *super-critical*, *critical* or *sub-critical* if k is > 1, $= 1$ or < 1, respectively. A nuclear reactor is maintained at $k = 1$ in order to have a steady state generation of neutrons and, hence, electricity.

$$k = \frac{\text{Number of neutrons in generation } (n+1)}{\text{Number of neutrons in generation } n} \tag{1.3}$$

Calculation of the multiplication factor k is based on following the life cycle of a neutron produced in fission, as is depicted in figure 1.3. Considering

first an infinite system, the multiplication factor is calculated by the *4-factor formula* in equation 1.4.

$$k_\infty = \eta\epsilon p f \tag{1.4}$$

η is the thermal fission factor which is defined as the ratio of the rate at which neutrons produced by thermal fission to the rate at which thermal neutrons are absorbed in the fuel:

$$\eta = \frac{\int\limits_{Cell}\int\limits_{0}^{E_c} \nu\Sigma_f\left(\vec{r},E\right)\phi\left(\vec{r},E\right)dEdV}{\int\limits_{Cell}\int\limits_{0}^{E_c} \Sigma_{aF}\left(\vec{r},E\right)\phi\left(\vec{r},E\right)dEdV} \tag{1.5}$$

Here, E_c is the boundary between the slowing down energy region and the thermal region (often taken to be 1 eV), ν is the average number of neutrons released in fission, Σ_{aF} is the macroscopic absorption cross-section for the fuel and $\phi\left(\vec{r},E\right)$ is the neutron flux density at energy E in the space point $\vec{r}$. The volume integration is performed over the unit cell.

ϵ is the fast fission factor, which is defined as the ratio of the total number of neutrons produced by *all* fission, to the number of neutrons produced in thermal fission:

$$\epsilon = \frac{\int\limits_{V_F}\int\limits_{0}^{\infty} \nu\Sigma_f\left(\vec{r},E\right)\phi\left(\vec{r},E\right)dEdV}{\int\limits_{V_F}\int\limits_{0}^{E_c} \nu\Sigma_f\left(\vec{r},E\right)\phi\left(\vec{r},E\right)dEdV} \tag{1.6}$$

Here, V_F is the fuel volume within a unit cell.

p is the resonance escape probability, which is defined as the probability that a neutron produced in fission will escape capture in the resonance energy region:

$$p = 1 - \frac{\int\limits_{Cell}\int\limits_{E_c}^{\infty} \Sigma_a\left(\vec{r},E\right)\phi\left(\vec{r},E\right)dEdV}{\int\limits_{Cell}\int\limits_{0}^{\infty} \Sigma_a\left(\vec{r},E\right)\phi\left(\vec{r},E\right)dEdV} \tag{1.7}$$

f is the thermal utilization factor, which is defined as the ratio of the thermal absorption rate in the fuel to the total thermal absorption

rate:

$$f = \frac{\int\limits_{V_F} \int\limits_{0}^{E_c} \Sigma_{aF}\left(\vec{r}, E\right) \phi\left(\vec{r}, E\right) dE dV}{\int\limits_{Cell} \int\limits_{0}^{E_c} \Sigma_{a}\left(\vec{r}, E\right) \phi\left(\vec{r}, E\right) dE dV} \tag{1.8}$$

For a real nuclear reactor, which is finite, k_∞ is modified to take into account neutrons which leak out of the reactor. For this correction, two factors $\Lambda_{f,t}$ denoting the probabilities that neutrons do *not* leak out while being fast (Λ_f) and thermal (Λ_t), respectively, are introduced. The multiplication factor for a finite system is thus written as:

$$k = k_\infty \Lambda_f \Lambda_t = \eta \epsilon p f \Lambda_f \Lambda_t \tag{1.9}$$

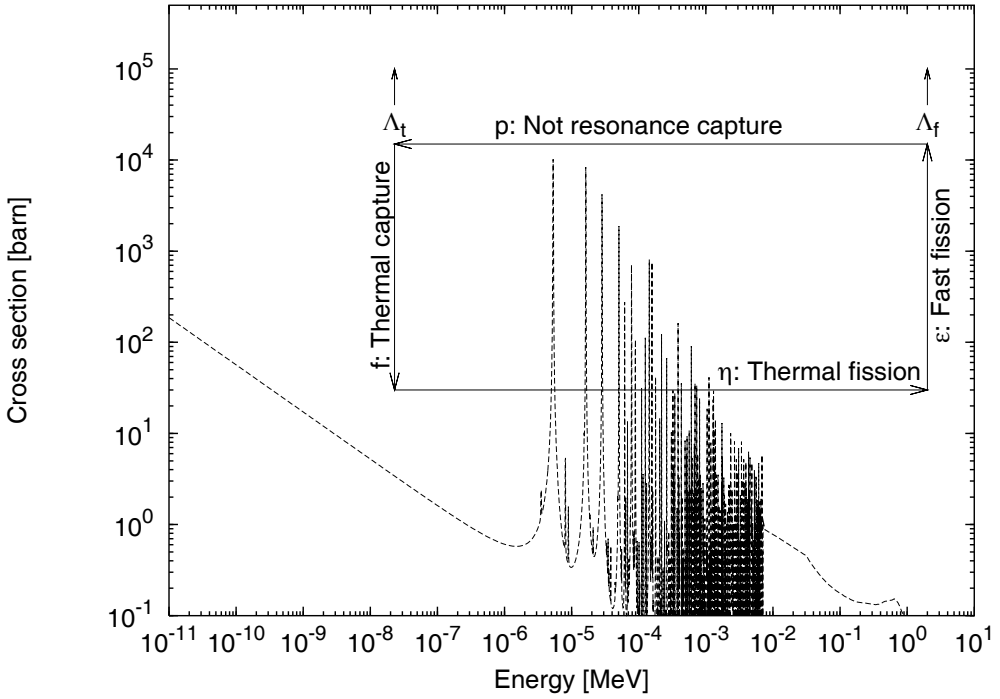

Figure 1.3: *The life cycle of neutrons in a nuclear reactor and factors used in the* 4-factor formula*, equation 1.9. Absorption cross-section data from figure 1.2 are included.*

Most light water reactors (LWR) in operation today are based on using uranium enriched to a few percent. The uranium fuel is normally placed in fuel rods that are distributed throughout the reactor core in a heterogeneous

pattern. The coolant, which also is the moderator, is flowing through the pattern of rods. The lumping of fuel into rods was first suggested by Fermi to increase the multiplication factor k. This increase is due to two reasons: 1) Fast fission neutrons will escape from the fuel and slow down by scattering in the moderator. Using appropriate spacing between the fuel rods, the neutrons are thermalized just before they enter into an adjacent rod where they may induce further fissions. 2) Neutrons that are slowed down to resonance energies near the surface of the fuel rods will be absorbed in the outer layers of the rod. This will decrease the neutron flux of resonance energy neutrons within the rod and, subsequently, the effective resonance absorption of the rod is reduced compared to that of an equivalent homogeneous mixture.

Since the purpose of the reactor is to produce heat, fuel rods used in a reactor should have a high thermal conductivity and a high melting point. Furthermore, the fuel should have a high resistance against radiation damage, corrosion and be chemically inert. For these reasons, the uranium based fuel is made of ceramic UO_2. To further enhance the mechanical stability of the fuel and to prevent fission products from escaping into the coolant, the UO_2 rods are encapsulated in a cladding of a Zirconium based alloy, which has a low neutron absorption cross-section and a good mechanical strength.

For safety reasons, as well as for control purposes, special control rods are used in the core. The control rods contain a highly neutron absorbing material such as boron, e.g. boron carbide B_4C powder, in order to control the multiplication factor of the core. In boiling water reactors (BWR), the control rods are made in the shape of a cross that fits in the center of four fuel assemblies. In pressurized water reactors (PWR), the control rods are placed in a number of positions in the fuel assembly.

A nuclear power plant is a highly complex installation which has been designed with great care. However, the principle of its operation is simple: The heat generated in the fission process is removed by a circulating coolant and subsequently used to generate steam which, in turn, is fed to a turbine system to produce electricity. This is illustrated in figure 1.4. In BWRs, steam is generated within the reactor core, which is fed to the turbine system. In PWRs, the pressure within the reactor vessel is so high that steam normally is not generated, instead the heated water is fed through a heat exchanger, where steam is generated and fed to the turbine system.

The control of the thermal power load in the core is performed in principle in the following manner:

1. During start-up, neutron absorbing control rods are removed from the core in sequences to enable the fission process to maintain a self-sustained chain reaction. The control rods are withdrawn from the bottom in a BWR (since steam used for electric generation is removed

from the top) and from the top in a PWR.

2. During the irradiation cycle, the power level is controlled by varying the flow of moderator/coolant through the core. In a PWR, the concentration of boron in the coolant is also used for controlling the fission rate.

3. During shut-down, the power level is naturally decreased when the criticality of the core drops below one. The fissionable material in the core has been consumed during the irradiation period and its concentration becomes too low to sustain the chain reaction.

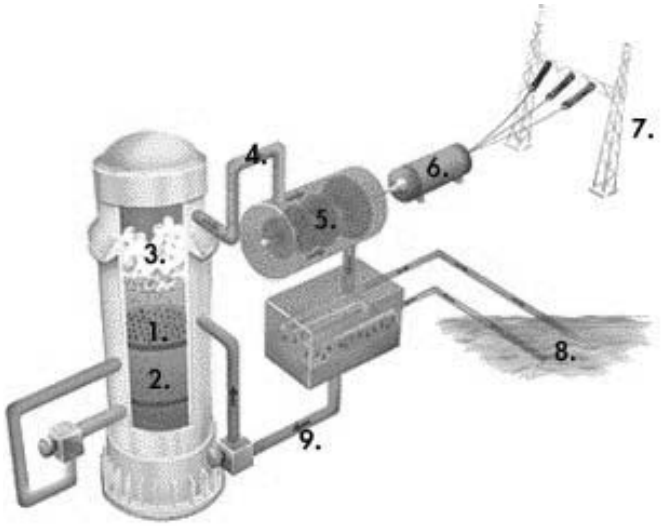

Figure 1.4: *The general principle of a nuclear reactor. 1) Core. 2) Control rods. 3) Steam. 4) Feed to turbine. 5) Turbine. 6) Generator. 7) Power grid. 8) Coolant intake. 9) Feedback to core from the condenser.*

1.2 The nuclear fuel cycle. Safety

The nuclear power industry in Sweden is based on the uranium-plutonium fuel cycle which is briefly described here in order to put the measurement techniques described in this thesis into context. Figure 1.5 summarizes the Swedish once-through[1] nuclear fuel cycle. Some nuclear fuel is manufactured within the country but it is not specifically targeted to the Swedish fuel

[1] Called "once-through" since no reprocessing is performed.

cycle. Also noted in the figure are points in the fuel cycle where techniques mentioned in this thesis have been studied.

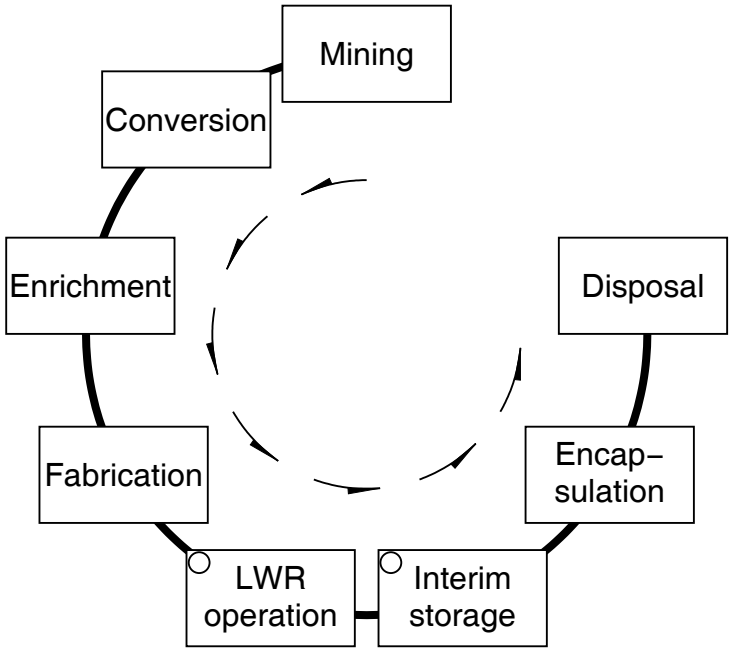

Figure 1.5: *The nuclear fuel cycle. The small circles mark where techniques mentioned in this thesis have been studied. This figure is based on information from ref. [7].*

Ore mining and fuel fabrication

The fuel used in the Swedish fuel cycle is made of uranium mined elsewhere in the world. Large uranium mining sites are currently to be found in Africa, Australia, Canada and USA. After the excavation, the uranium is converted into uranium hexafluoride, UF_6. The ^{235}U content in UF_6 is enriched to a few percent, compared to the fraction in natural uranium that contains about 0.72% ^{235}U and 99.27% ^{238}U [8]. The enriched UF_6 forms the basis of fabrication of UO_2 ceramic and sintered pellets which eventually are put into fuel rods. These rods are combined into fuel assemblies, see figure 1.6. As an example, Westinghouse Atom AB in Sweden produces about 400 tons of UO_2 fuel for LWRs per year [9].

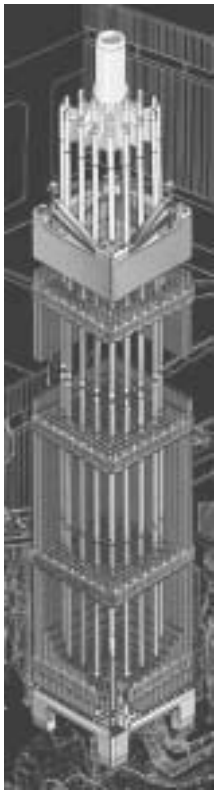

Figure 1.6: *Sketch of a PWR nuclear fuel assembly from Westinghouse, courtesy of ref. [10].*

In-core utilization of the fuel

In Sweden, eleven nuclear power reactors are in operation at the time of this writing, eight BWRs and three PWRs. The total power installed is 9819 MW_e and the annually production of electricity from nuclear power is 54.8 TWh[2] or about 45% of the total amount produced. This electricity production results in 150-200 tonnes of spent fuel annually.

While the fuel is irradiated in the core and shortly afterward, the heat produced in the fuel must of course be adequately cooled off by means of the coolant/moderator. Even after long cooling times, the produced decay heat can still be significant. The decay heat is further discussed in sections 2.1.3 and 4.1.2.

In the Swedish nuclear fuel cycle, the fuel is typically irradiated in the reactor core during 3-6 cycles, with irradiation periods of about 10-11 months. Between each irradiation period, there is a shutdown period when re-fueling,

[2]During the year 2000. From Statistics Sweden, Statistical Notices.

re-ordering of fuel bundles within the core, and maintenance of the reactor and other systems are performed.

Spent fuel management

The nuclear fuel removed from the reactor core after irradiation is stored at the reactor site and cooled for about one year after which it is transported to the interim storage CLAB in Oskarshamn, Sweden. The spent fuel is stored temporarily in CLAB for about 30 to 40 years before transportation to the site of the final storage. Here, the fuel will be encapsulated and stored in a deep geological repository [11]. At all stages during the process, a high level of security as well as safety is of great importance.

1.3 Scope of the thesis

For reasons of safety and efficiency, knowledge of the behavior and characteristics of the nuclear fuel during operation is needed. Also, in all storage locations in the nuclear fuel cycle, the properties of the fuel must be adequately known in order to obtain a safe and secure storage. Characterization of the fuel is therefore needed throughout the fuel cycle.

Computer codes are normally used to calculate the characteristics of the nuclear fuel. The very strong demands put on the quality of the calculated results necessitate experimental validation and verification of the codes for the nuclear operation, for the interim storage and for the encapsulation plant. Further on, safeguard issues raise the need for verification of calculations of the fissile contents in the fuel.

The measurement techniques presented in this thesis have been developed with the goal to determine, with high accuracy, various parameters of the nuclear fuel. Non-destructive measurement methods utilizing radiation emitted from the fuel are shown to be valuable tools for characterization of nuclear fuel. Specifically, methods have been developed for accurate determination of the thermal power distributions in nuclear fuel assemblies by gamma-ray tomography. Also, methods have been developed for determination of burnup, the decay heat and fission gas release in a fuel assembly by means of gamma-ray spectroscopy.

Chapter 2

The nuclear fuel

The nuclear fuel cost is a major expense in nuclear power, representing about 15-20 % of the total cost of generating electricity from nuclear power, see ref. [12]. Therefore, substantial efforts are put into optimizing the performance of the fuel, in order to maximize the power output within safety limits. Various improvements regarding physical dimensions of the fuel, cladding and spacers are a continuing effort among fuel producers. Also, the composition of the material in various components of the fuel is an important research area. With increasing competition on the power generation arena, the need for more efficient and accurate characterization methods is increasing as well.

In this chapter some parameters of the nuclear fuel are defined. Further on, the radiation emitted from the fuel, that may be used for characterization of the parameters defined, is discussed.

2.1 Some fuel parameters and their significance

Several parameters of the fuel are of interest both for general characterization, e.g. in conjunction with core physics calculations, and for verifying irradiated fuel, which is a concern of the international safeguards. In this section such parameters will be presented and discussed to some extent.

Verifying parameters of an assembly such as burnup and cooling time (which will be defined later on in this section) is an important task for safeguard inspectors since a falsified or erroneous declared value may indicate activities at the facility that have not been accounted for, e.g. handling of fissile material outside the scope of the safeguards agreement.

Values of some of the fuel parameters such as burnup, decay heat and concentrations of various isotopes in the fuel matrix can be obtained from calculations. In such calculations, a homogeneous model of the nuclear fuel

Parameter and notation used in this thesis	Values
enrichment (ε)	1.5-4 wt%
void history	~50 % (BWR)
burnup (β)	20-50 GWd/tU
power history	3-6 cycles
cooling time (T)	0-50 years
decay heat (P)	0.1-1 kW (BWR)

Table 2.1: *Some fuel parameters and typical values in Swedish nuclear fuel.*

is often used in order to simplify the procedure. The time dependence of isotope production and depletion in a homogeneous medium is calculated by developing solutions to equation 2.1, where N_i is the concentration of a particular nuclide i.

$$\frac{dN_i}{dt} = \text{Formation Rate} - \text{Destruction Rate} - \text{Decay Rate} \tag{2.1}$$

When the right hand side of equation 2.1 contains radioactive disintegration and neutron capture and fission, the time rate of change of a nuclide i is written as:

$$\frac{dN_i}{dt} = \sum_j \gamma_{ji}\sigma_{f,j}N_j\phi + \sigma_{c,i-1}N_{i-1}\phi + \lambda_i' N_i' - \sigma_{f,i}N_i\phi - \sigma_{c,i}N_i\phi - \lambda_i N_i \tag{2.2}$$

Here,

- $\left(\sum_j \gamma_{ji}\sigma_{f,j}N_j\phi\right)$ is the yield rate of N_i due to the fission of all nuclides N_j,
- $(\sigma_{c,i-1}N_{i-1}\phi)$ is the rate of transmutation into N_i due to capture in N_{i-1},
- $(\lambda_i' N_i')$ is the rate of production of N_i due to decay of N_i',
- $(\sigma_{f,i}N_i\phi)$ is the destruction rate of N_i due to fission,
- $(\sigma_{c,i}N_i\phi)$ is the destruction rate of N_i due to other forms of capture: (n,γ), (n,α), (n,p), (n,2n) and (n,3n),
- $(\lambda_i N_i)$ is the decay rate of N_i.
- γ_{ji} is the fission yield,
- σ_f is the microscopic fission cross-section,

- σ_c is the microscopic capture cross-section,
- N_i is the concentration of a particular nuclide i,
- ϕ is the space-energy-averaged neutron flux density,
- λ_i is the decay constant of nuclide i,

Several codes exist which solve equation 2.2, see e.g. refs. [13, 14]. In this work, calculations have been performed using the ORIGEN computer code, developed at Oak Ridge National Laboratory (USA). This code is capable of calculating the dynamics of the isotope production and depletion as the fuel is irradiated in the reactor. The code is part of the SCALE package [15] which is used in computer analyses for licensing.

In ORIGEN, a space-energy-averaged neutron flux density ϕ is used together with flux density-weighted averaged cross-sections σ_f and σ_c in order to solve equation 2.2 for a homogeneous medium. Equation 2.2 is the basis of a system of first-order linear differential equations and is solved in ORIGEN by the matrix exponential method, in which the time evolution is calculated by discretizing the time in small time intervals Δt. The neutron flux density and the cross-sections are assumed to be constant during Δt. The flux density and cross-sections may, however, be updated between the time intervals in order to take into account parameters that are not included in the homogeneous model, e.g. lattice effects and void.

The ORIGEN code uses condensed cross-sections in a homogeneous model, which implies that the calculation of the integrated cross-sections is a source of uncertainty in the model. Furthermore, the uncertainties of the basic cross-sections add further uncertainty to the final result. Ref. [16] reports results from validations performed with the code; for most nuclides in the isotopic inventory, the uncertainties were in the order of 5%. For some actinides, e.g. americium, curium and neptunium, the uncertainties were in the order of 20%. Updating the condensed cross-section libraries with new data is an on-going effort pursued by the ORIGEN code developers [17].

2.1.1 Burnup

Burnup (β) is a measure of the amount of energy produced in the fuel and two definitions are used: 1) The number of fissions per 100 heavy nuclides (with mass number ≥ 232) initially present in the fuel, expressed in percent. 2) The integrated energy release from fission of initially present heavy nuclides, usually expressed in the unit GWd/tU. The two definitions are related through a factor describing the effective energy released per fission, i.e. about 200 MeV, as indicated in equation 2.3.

The first definition is often used for dissolved irradiated fuel while the second definition is used in non-destructive assay (NDA) of spent fuel and for power reactors. Typical values on the burn-up are displayed in table 2.1. The burnup can be obtained from measurements of the concentration of a fission product as suggested by equation 2.3.

$$\beta = E \cdot \frac{N}{Y} \tag{2.3}$$

where

N is the number of nuclei produced during irradiation per mass of initial heavy metal, of the selected burnup indicator.

Y is the average fractional fission-yield.

E is the average energy released per fission.

N/Y is the number of fission events during irradiation, per mass of initial heavy metal.

The number of nuclei N, i.e. the concentration of a fission product, may be measured using gamma-ray spectroscopy, whereby the intensity of gamma-rays emitted from the fission product is a measure of the concentration. This procedure will be further discussed in chapter 4.

For safeguard purposes, the principal goal of spent fuel assay is to determine the contents of fissile materials in the bundle. The fissile content, e.g. the concentration of Pu, is related to the burnup of the fuel, therefore non-destructive techniques for experimental determination of the fuel burnup are important features of the IAEA safeguards.

2.1.2 Cooling time

The cooling time of a nuclear fuel assembly is defined as the time elapsed since the end of the last irradiation.

The cooling times encountered in this work, during measurements performed on Swedish spent fuel, range from a few months to up to about 20 years. This can be compared to the expected cooling time of 30-50 years at the time when the fuel is to be encapsulated for deep geological storage.

2.1.3 Decay heat

Radioactive isotopes are produced by the neutron irradiation of the fuel during operation. The decaying isotopes within the fuel matrix produce decay heat due to absorption of particles and electromagnetic radiation emitted in

the radioactive decay. The decay heat can be calculated using, for instance the ORIGEN code [18, 19]. Figure 2.1 shows time evolution of the decay heat produced in a typical BWR fuel assembly.

As indicated in figure 2.1, the residual thermal power in a typical BWR assembly drops from about 75 kW to about 0.2 kW between one hour and 40 years of cooling time. For a PWR assembly, the residual thermal power follows the same behavior as for a BWR bundle but is scaled by roughly the mass of the fuel, i.e. about a factor of 3.

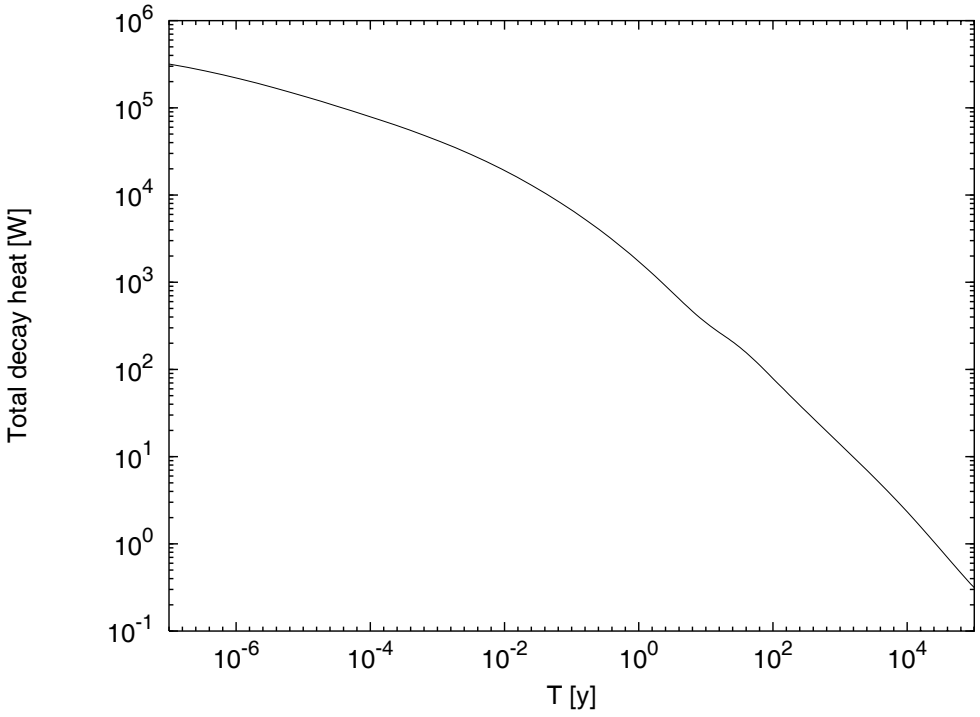

Figure 2.1: *The time evolution of decay heat produced in a nuclear fuel assembly. Calculated with ORIGEN-S [19] for a BWR 8×8 fuel assembly with 3% initial ^{235}U enrichment and with burnup 40 GWd/tU distributed equally over four fuel cycles.*

A summary of the most important contributions to the decay heat for fuel with cooling time above ten years, calculated using the ORIGEN code, is shown in table 2.2. Some elements are long-lived and contribute to the decay heat for decades while other elements dominate the decay heat at short cooling times up to a few years.

After about 40 years of cooling time, i.e. at the time when encapsulation is expected, heavy elements and actinides produced in the irradiation process

T [y]	10	15	20	25	30	35	40	45	50
^{90}Sr	5.3	5.5	5.4	5.2	5.1	4.9	4.7	4.5	4.3
^{90}Y	25.3	26.0	25.6	24.9	24.1	23.3	22.4	21.5	20.6
^{134}Cs	4.9	1.1	0.2	0.0	0.0	0.0	0.0	0.0	0.0
^{137}Cs	7.8	8.1	8.0	7.9	7.7	7.5	7.2	7.0	6.8
^{137}Ba^m	26.1	27.0	26.8	26.3	25.6	24.9	24.2	23.4	22.5
^{154}Eu	2.4	1.8	1.4	1.0	0.7	0.5	0.4	0.3	0.2
^{238}Pu	8.8	9.8	10.5	11.1	11.7	12.3	12.9	13.4	13.9
^{239}Pu	0.7	0.8	0.9	0.9	1.0	1.1	1.2	1.3	1.4
^{240}Pu	1.3	1.6	1.8	1.9	2.1	2.3	2.5	2.7	3.0
^{241}Am	4.6	7.0	9.3	11.4	13.5	15.6	17.6	19.7	21.8
^{244}Cm	10.8	10.4	9.5	8.6	7.8	7.1	6.3	5.7	5.1

Table 2.2: *Main contributors to the decay heat as a function of cooling time (T), in percent. Calculated with ORIGEN-S [19] for a BWR 8×8 fuel assembly with 3% initial ^{235}U enrichment and with burnup 40 GWd/tU distributed equally over four fuel cycles.*

contribute by about 40% to the decay heat, mostly due to α decay, and this contribution increases with time due to their long half-lifes. Fission products contribute with about 60% to the decay heat, mostly by means of β decay and γ de-exciation. This contribution decreases with time. Elements produced from irradiated construction materials in the fuel, e.g. ^{60}Co, do not contribute significantly to the decay heat.

2.1.4 Void fraction

Void fraction is defined as the volume fraction of the coolant (water in LWR reactors) in the gas phase. The presence of void is a typical design feature of BWRs. The mass density (ρ) of the mixture between a liquid coolant and a coolant in the gas phase can be written as $\rho = \rho_g\alpha + \rho_l(1-\alpha)$ where α is the void fraction, ρ_g is the mass density of the gas and ρ_l is the mass density of the liquid. For a BWR operating at 70 bar, the values of ρ_g and ρ_l are about 37 kg/m^3 and 740 kg/m^3 respectively. The void fraction is often summarized as an average value of the entire irradiation time. The average value is then called "void history". Typically, the void history value is about 50%.

The relatively large span of void fractions possible in a BWR implies a large effect on the moderating conditions and consequently a large effect on the build-up of plutonium, burning of fissile material and the build-up of fission products. Uncertainties attributed to the void fraction is one of the main contributions to the total uncertainty obtained in reactor core calculations

of e.g. power distribution, in and reactivity of, the fuel assembly.

2.1.5 Enrichment

The initial enrichment is defined as the fraction of uranium atoms that consist of ^{235}U in the fuel matrix. It is usually expressed in percent by weight. The uranium of the fuel is enriched in ^{235}U to between 1.5-4 percent by weight as compared to natural uranium that contains 0.72% ^{235}U and 99.27% ^{238}U [8]. Current development of nuclear fuel is aiming at higher enrichments to meet increasing demands of energy out-take per fuel element. The world-wide average enrichment is predicted to increase from 3.35 % in 1990 to 3.85 % by the year 2010 [20].

The initial enrichment is an important variable parameter when designing nuclear fuel bundles. The rate of build-up and burning of fissile material in the fuel matrix is strongly dependent on the shape of the neutron spectrum, which in turn depends strongly on the distribution of void (in BWR reactors) and the control rods. A careful design of the distribution of enrichment, makes it thus possible to obtain a more homogeneously distributed power out-take compared to the case with constant enrichment.

2.1.6 Irradiation history

The irradiation history of a fuel assembly is defined as the burnup as a function of time, while the fuel assembly was in the reactor core. If the nuclear fuel has been subject to an unusual irradiation history, e.g. if it has been irradiated in a low flux density of neutrons for long periods, the production rate of e.g. plutonium is higher than during normal irradiation periods. The ability to detect such an unusual irradiation history is valuable for international safeguards. This is discussed briefly in section 4.1.1.

2.1.7 Contents of fissile materials

Initially, the fuel consists of UO_2. During irradiation, processes such as neutron capture and β- and α-decay produce various concentrations of fissile material, depending on parameters such as irradiation history, neutron energy spectrum and void fraction in the core. Figure 2.2 shows the mass of ^{235}U and ^{239}Pu as a function of time in a typical BWR fuel assembly.

2.1.8 Fuel integrity

Fuel integrity is important for two reasons. First, it is important that the fuel rods remain intact during fuel handling and during operation in the reactor

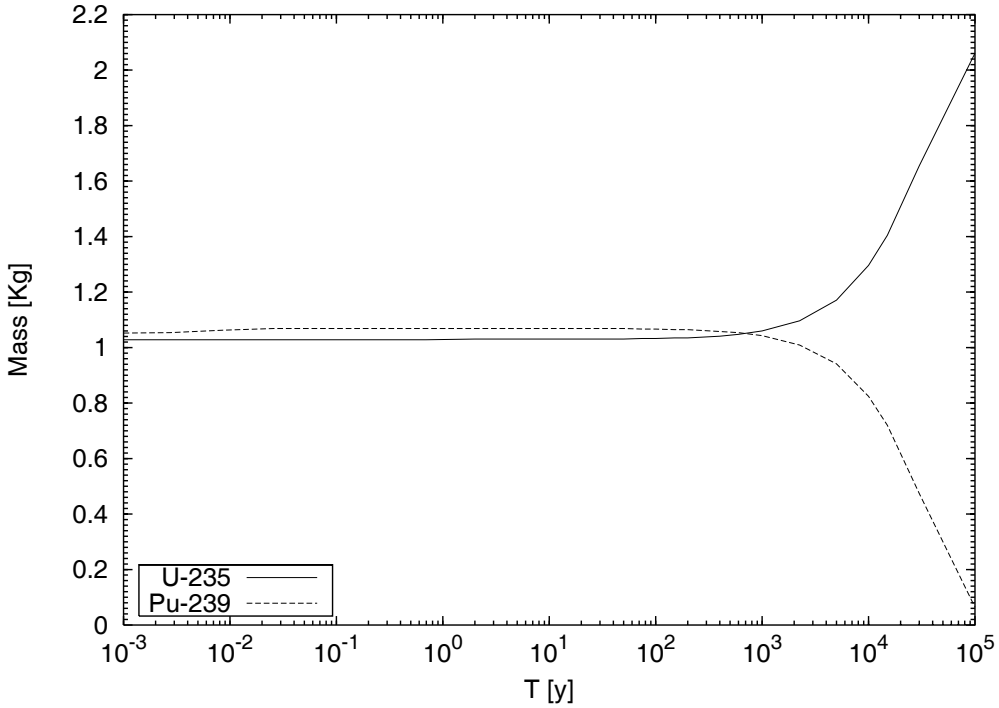

Figure 2.2: *The time evolution of the mass of the fissile isotopes ^{235}U and ^{239}Pu in a nuclear fuel assembly. Calculated with ORIGEN-S [19] for a BWR 8×8 fuel assembly with 3% initial ^{235}U enrichment and with burnup 40 GWd/tU distributed equally over four fuel cycles.*

core. Second, it is a significant effort for safeguards authorities to verify the completeness of fuel rods in a fuel assembly against operator declared data. In this work, the term *integrity* is used in connection to the second reason, when discussing missing rods in a fuel assembly.

IAEA Safeguards Criteria [21] use the term *defect* as the "difference between the declared amount of nuclear material /.../ and the actual amount present". Three types of defects are specified:

1. *Gross defect* for a nuclear assembly for which the declared data have been falsified to the maximum extent possible, i.e. with all rods missing or replaced by dummys.

2. *Partial defect* when a considerable fraction of the fuel rods are wrongly declared.

3. *Bias defect* when a small fraction is wrongly declared, e.g. a few individual rods in a fuel assembly are missing or replaced.

Measurement methods for verifying fuel integrity of the partial and bias defect level have been developed during the course of this work. These are further discussed in sections 4.2.2 and 4.3.

2.2 Nuclear fuel as a radiation source

The isotopes of uranium are weakly radioactive and decay via α-decay and spontaneous fission with long half lives: $7{\cdot}10^8$ y and $4.5{\cdot}10^9$ y for ^{235}U and ^{238}U, respectively [8]. During irradiation, processes such as fission and neutron capture reactions produce many radioactive isotopes, see for example figure 2.3. Most of the fission products produced have short half lives and decay within a few seconds. Some fission products, though, have life-times ranging from the order of days up to several years and decades. See table 2.3.

After irradiation, no direct buildup of radioactivity takes place and the total radioactivity decreases with time. Some radioactive isotopes are still produced, however, mainly via decay. As an example, figure 2.3 shows the activity of various isotopes as a function of time in a typical BWR assembly as calculated using ORIGEN-S.

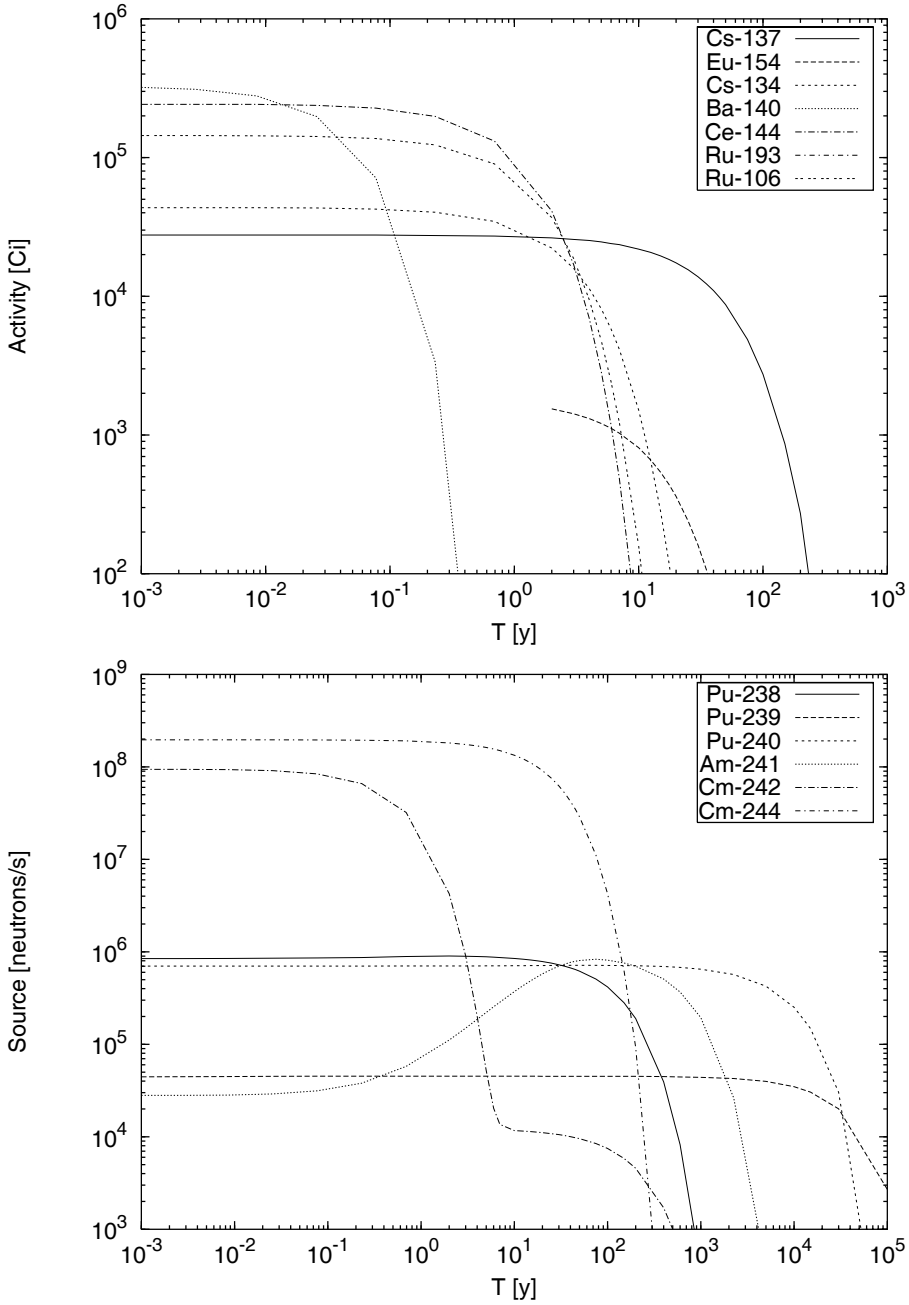

Figure 2.3: *The time evolution of some gamma activities (top) and neutron sources (bottom) in a BWR nuclear fuel assembly. Calculated with ORIGEN-S [19] for a BWR 8×8 fuel assembly with 3% initial ^{235}U enrichment and with burnup 40 GWd/tU distributed equally over four fuel cycles.*

2.2.1 Gamma radiation

During irradiation, a vast number of fission products are produced in the fuel matrix. In practice, however, only a few are of interest for diagnostic purposes, since most of the fission products have short half lives. Table 2.3 lists some isotopes that emit gamma-radiation, together with their fission yield. The activities of these isotopes in a typical fuel assembly are shown in figure 2.3.

Within the order of days up to a year after irradiation, the isotopes ^{95}Nb, ^{95}Zr, ^{103}Ru, ^{106}Ru, ^{140}Ba and ^{144}Ce are available for measurement. Years after irradiation, the short-lived isotopes have decayed and the gamma-ray spectrum is dominated by ^{134}Cs, ^{154}Eu and ^{137}Cs.

The production path and decay scheme of some of the isotopes displayed in table 2.3 are shown in figures 2.4 and 2.5. Decay schemes for some isotopes are shown in figure 2.6. The isotopes ^{95}Zr, ^{106}Ru, ^{137}Cs, ^{140}Ba and ^{144}Ce are produced directly from the beta decay of precursor fission products, see e.g. the path for ^{137}Cs. This is not the case of ^{134}Cs and ^{154}Eu since they are only to a small extent produced directly from fission. The cumulative thermal fission yields of ^{137}Cs and ^{154}Eu are $6.19{\cdot}10^{-2}$ and $1.94{\cdot}10^{-9}$ per fission, respectively [4]. For ^{134}Cs, the thermal fission yield is negligible. Instead, the production involves series of (n,γ) reactions and beta decays, as shown in the figures. Due to their relatively complex way of production, the buildup of ^{134}Cs or ^{154}Eu is dependent on the neutron spectrum in the reactor and thus on the initial enrichment of the fuel and void.

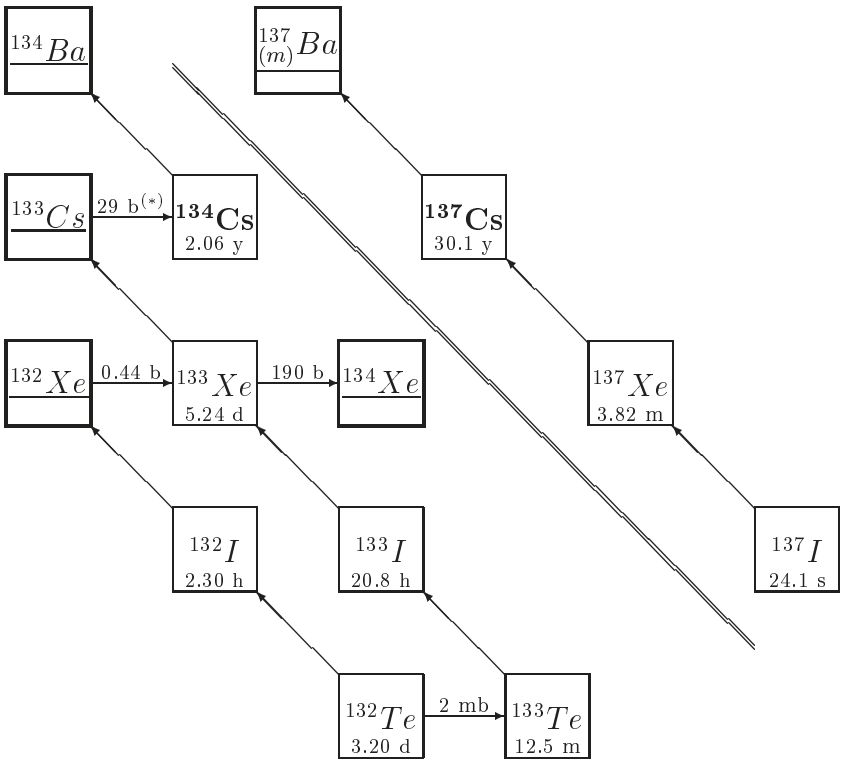

Figure 2.4: *Main production path and decay chain for* ^{134}Cs *and* ^{137}Cs*. Half-lifes are from [8] and thermal (2200 m/s) neutron-capture cross-sections, printed on top of the horizontal arrows, are from [24]. Stable isotopes are underlined.*
(*) *The resonance integral cross-section in* ^{133}Cs *of 421 barns [24] is a significant contribution to the production of* ^{134}Cs*.*

Isotope	$T_{1/2}$	Thermal Fission Mass Yield			Principal Gamma Rays		Attenuation [cm^{-1}]	
		^{233}U	^{235}U	^{239}Pu	Energy [keV]	Branching [%]	UO_2	H_2O
^{95}Nb	34.975(8) d	6.3	6.50	4.81	765.8	100.0	1.078	0.080
^{95}Zr	64.02(5) d	-"-	-"-	-"-	235.7	0.3	8.313	0.129
					724.2	44.0	1.152	0.082
					756.7	54.0	1.099	0.080
^{103}Ru	39.26(2) d	1.57	3.03	7.0	497.1	91.0	1.947	0.097
					610.3	6.8	1.445	0.089
^{106}Ru $\rightarrow ^{106}$Rh$^{(*)}$	373.59(15) d	0.25	0.401	4.3	511.8	20.0	1.864	0.096
					621.9	10.0	1.403	0.088
					1050.4	1.6	0.770	0.069
					1128	0.4	0.719	0.066
					1562.2	0.2	0.566	0.056
^{134}Cs	2.065(1) y	6.30	6.87	7.68	563.2	8.4	1.612	0.092
					569.3	15.0	1.591	0.091
					604.7	98.0	1.455	0.089
					795.9	86.0	1.031	0.079
					802	8.7	1.023	0.078
					1365.2	3.0	0.617	0.060
^{137}Cs	30.07(3) y	6.81	6.19	6.62	661.7	85.0	1.298	0.086
^{140}Ba $\rightarrow ^{140}$La$^{(*)}$	12.752(3) d	6.4	6.21	5.38	815.8	23.0	1.003	0.078
					925.2	6.9	0.874	0.073
					1596.2	95.0	0.560	0.056
					2521.4	3.5	0.471	0.043
^{144}Ce $\rightarrow ^{144}$Pr$^{(*)}$	284.893(8) d	4.68	5.50	3.74	696.5	1.3	1.215	0.084
					1489.2	0.3	0.582	0.058
					2185.7	0.7	0.490	0.047
^{154}Eu	8.593(4) y	0.047	0.074	0.262	591.8	5.0	1.508	0.090
					723.3	20.0	1.152	0.082
					873.2	12.0	0.930	0.075
					996.3	11.0	0.810	0.071
					1004.7	18.0	0.804	0.070
					1274.4	35.0	0.648	0.062

Table 2.3: *Various isotopes that be may used in γ-ray measurements on nuclear fuel. Half-lifes are from [8], fission yields are from [22], γ-ray energies and branching are from [8] and attenuation coefficients are from [23] (the total attenuation, with coherent scattering, is given).* $^{(*)}$ *The half-lifes for* ^{106}*Rh,* ^{140}*La and* ^{144}*Pr are 29.80(8) seconds, 1.6781(3) days and 17.28(5) minutes, respectively.*

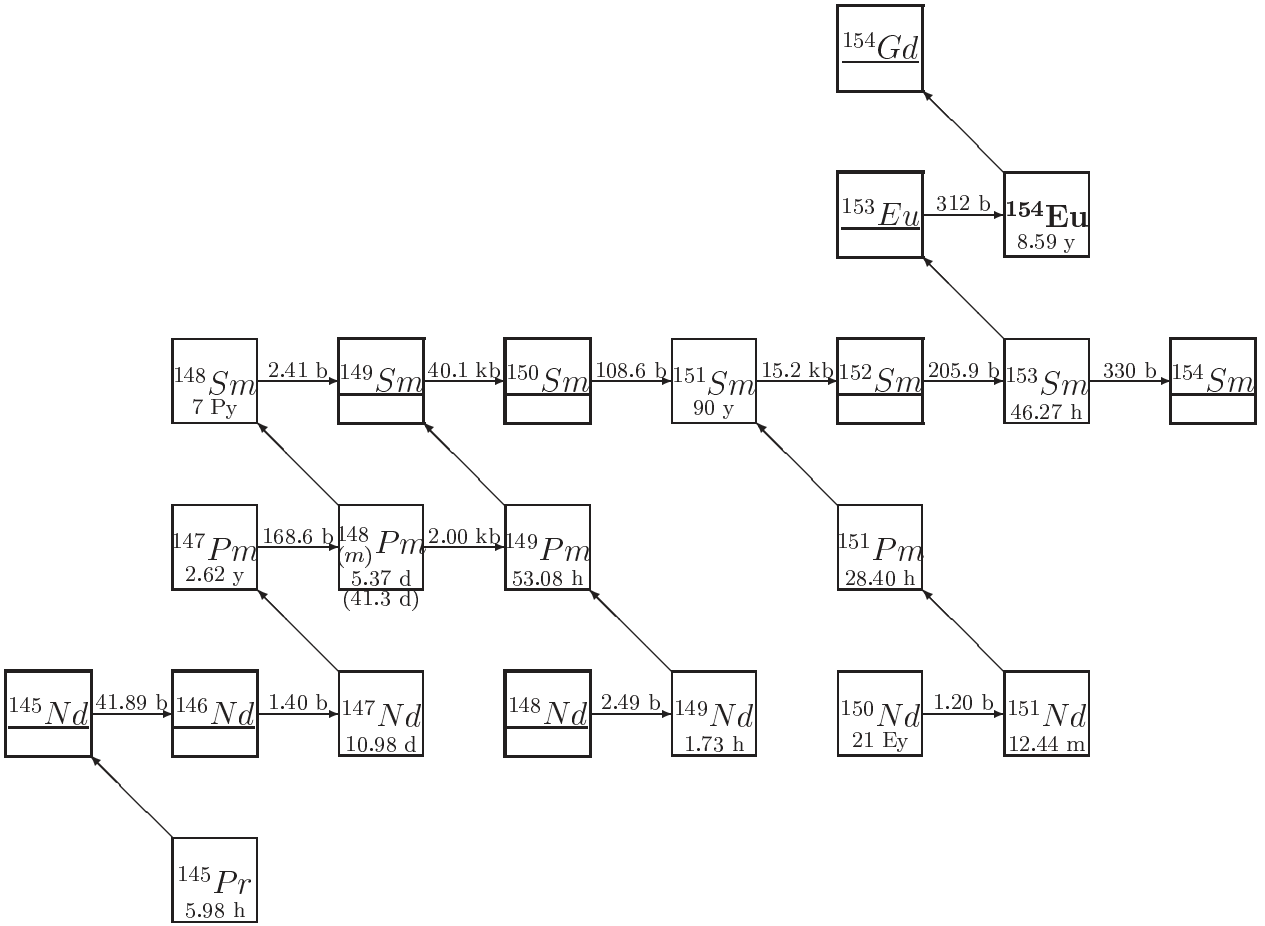

Figure 2.5: *Main production paths for ^{154}Eu. The half-life for $^{148}Pm^{m}$ is indicated within parenthesis. Half-lifes are from [8] and thermal (2200 m/s) neutron-capture cross-sections, printed on top of the horizontal arrows, are from [24]. Cross-sections for $^{146,148,150}Nd$, $^{148,150}Sm$ and ^{148}Pm are from [25]. Stable isotopes are underlined.*

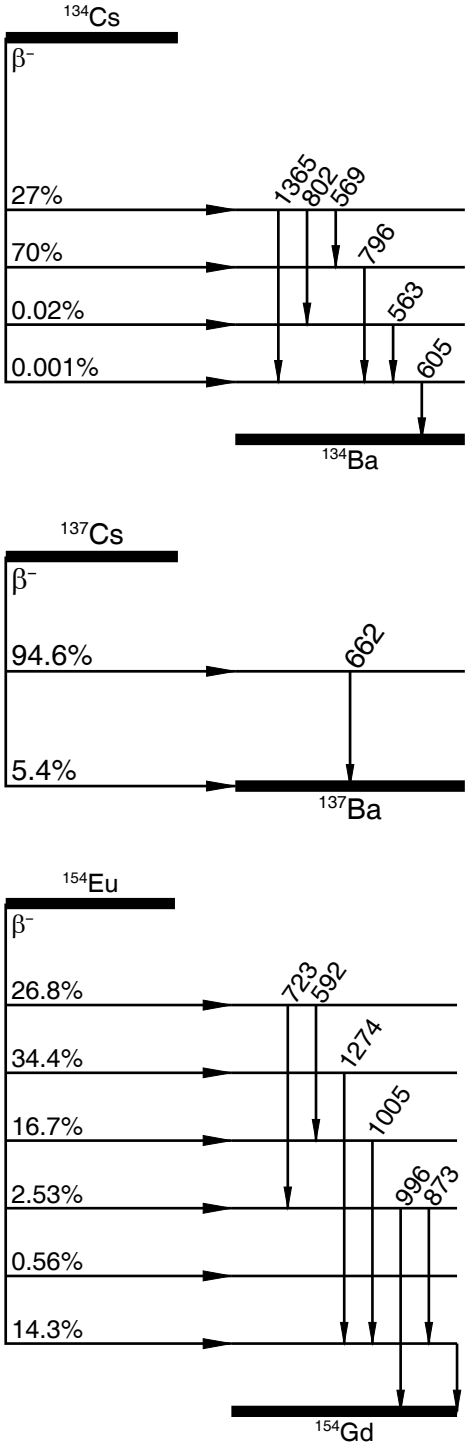

Figure 2.6: *Decay schemes for some gamma emitters encountered when performing measurements on nuclear fuel. Only the energies listed in table 2.3 are given, (in keV).*

2.2.2 Neutrons

In the spent fuel matrix, three reaction types are the main sources of neutrons: Spontaneous fission, induced fission and (α,n) reactions. Other reactions such as (n,2n) and (γ,n) are also possible but contribute less due to small cross-section.Table 2.4 shows concentrations of the most common neutron emitting isotopes in typical spent fuel.

Figure 2.8 shows the major production paths of transuranic isotopes in the fuel matrix. The neutron signal from spent fuel is dominated by neutrons from isotopes of curium. Shortly after shutdown of the reactor, the most significant neutron emitter is ^{242}Cm and after several years of cooling the neutron source is dominated by ^{244}Cm. These two isotopes emit neutrons by means of spontaneous fission for which the energy distribution $f(E)$ of the emitted neutrons often is described by Watt's function according to equation 2.4, where a and b are parameters, specific for each isotope as shown in table 2.4. Figure 2.7 shows Watt's distribution for some isotopes.

$$f(E) = Ce^{-E/a} \sinh\left(\sqrt{bE}\right) \tag{2.4}$$

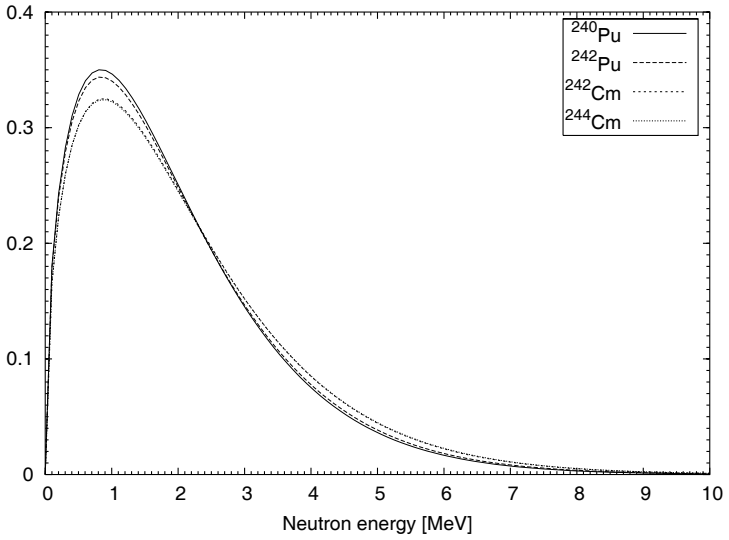

Figure 2.7: *The spontaneous fission neutron energy spectrum according to equation 2.4, for some isotopes. The energy spectra $f(E)$ have been normalized so that $\int_0^\infty f(E)dE = 1$.*

Isotope	$T_{1/2}$	a	b	C	Neutron-rates [s^{-1}]	
		[MeV]	[MeV^{-1}]		Spont. fission	(α,n)
^{240}Pu	6.56(2) ky	0.799	4.903	0.268	$6.2{\cdot}10^5$	$9.3{\cdot}10^4$
^{242}Pu	373.3(12) ky	0.834	4.432	0.279	$3.0{\cdot}10^5$	$3.8{\cdot}10^2$
^{242}Cm	162.8(2) d	0.891	4.046	0.271	$8.8{\cdot}10^3$	$1.8{\cdot}10^3$
^{244}Cm	18.10(2) y	0.906	3.848	0.279	$6.2{\cdot}10^7$	$4.7{\cdot}10^5$

Table 2.4: *Typical neutron sources in nuclear fuel. Half-lifes are from [8]. Parameters a and b for Watt's fission energy spectrum $f(E)$ for spontaneous fission of some isotopes, from [26]. The normalization parameter C was calculated so that $\int_0^\infty f(E)dE = 1$. The spontaneous fission and (α,n) rates in a typical BWR with a cooling time of 30 years are shown. Calculated with ORIGEN-S [19] for a BWR 8×8 fuel assembly with 3% initial ^{235}U enrichment and with burnup 40 GWd/tU distributed equally over four fuel cycles.*

Figure 2.8: *Main production paths and decay chain for the transuranic elements most commonly found in the nuclear fuel matrix. Half-lifes are from [8] and thermal (2200 m/s) neutron-capture cross-sections, printed on top of the horizontal arrows, are from [25].* (*) *The two first isomers of* ^{242}Am *have half lives of 141 y and 14.0 ms, respectively.*

Chapter 3

Measurement techniques

3.1 Gamma radiation detector systems

In general, high count rates may be preferred for two reasons in gamma-ray spectroscopy measurements: 1) Measuring weak activities in the presence on strong peaks may require a high count rate. 2) Limited time to perform the experiment may require fast counting. Specifically, for studies of nuclear fuel, both reasons are often the case.

3.1.1 Detectors

Two types of gamma radiation detectors are widely used in the field of non-destructive assay of nuclear fuel: Scintillation detectors (e.g. NaI(Tl) or BGO) and semiconductor (e.g. high-purity germanium) detectors.

In this thesis, two applications involving gamma-ray measurements are described (in chapter 4): Gamma scanning and tomography. For the first application, the intensity of the gamma-ray flux density from certain isotopes is measured using high-resolution gamma-ray spectroscopy. High energy resolution is often needed in this case due to a relatively complex energy spectrum. A germanium detector has therefore been used in this application.

In the second application, the energy spectra measured are dominated by one peak (from ^{140}Ba at 1596 keV), implying that a smaller and less expensive scintillation detector can be used. Peak efficiencies of scintillation detectors are comparable to germanium detectors and the count rates that may be achieved using a scintillation detector system are at least as high. In the tomography application, the detectors are placed relatively close to the fuel assembly, implying a varying temperature of the detectors. Therefore, special attention was paid in order to measure and stabilize the temperature.

Both applications are subject to time constraints, set by the nuclear fa-

cility, which imply that the measurements need to be performed using a high count rate system. This imposes constraints on the type of electronics and data acquisition system used.

A third application also involves high-resolution gamma-ray spectroscopy. A large Compton background can, in cases where the peaks of interest are very weak, make the peak evaluation more uncertain. The anti-Compton suppression system described in paper I utilize a set of scintillation detectors, surrounding a high-resolution germanium detector. By measuring the pulses from the scintillation detectors in coincidence with the germanium pulses and using that coincidence as a veto against pulses in the germanium detector, a suppression of the Compton background is established. This implies that peaks that are barely visible without the suppression are enhanced, thus reducing the uncertainty of the peak evaluation.

3.1.2 Electronics and data acquisition systems

There are several criteria regarding the properties and/or the performance of the electronics and data acquisition system used for the applications mentioned in this work:

- The data acquisition system should be portable or easy transportable to facilitate measurements at nuclear facilities which often have restrictions on transporting items in and out from the facility.
- High count rates have been the priority due to limited time to perform experiments. Time constraints are set either by the operator of the facility (in order not to interfere with the normal facility routines) or by safety regulations regarding handling of nuclear fuel.
- Energy resolution of the detector system should be appropriate for the application.

In the early part of the work, electronics and data acquisition systems was based on the Nuclear Instrumentation Module (NIM) standard. In papers I, II and III, the NIM standard has been used. Following, is a list comprising essential features of the NIM-units used:

- Pre-amplification of the signals was performed using a transistor-reset amplifier which allows for high count rates.
- Amplification with the gated integrator method[1] was performed, also in order to allow for high count rates.

[1]Model: Ortec 973U.

- Analog-To-Digital conversion was done using an ADC with a fixed conversion time[2]. This type of ADC has a fixed deadtime.

- A pulse generator with a frequency of 2 kHz was used for dead time correction, see section 3.1.3. The relatively low frequency of pulses was about one percent of the total count rate and did not contribute significantly to the system dead time.

- A specially designed PC-card interface[3] was used to collect and store data from the ADC with on-line display of gamma-ray measurement results. This card is capable of storing spectra into computer memory at count rates exceeding 200 kcps [27].

The features of the data acquisition system as described above allows for a throughput of over 100 kcps with an energy resolution of about 3 keV FWHM of the ^{137}Cs peak at 662 keV. A typical electronic setup based on this system and used for gamma scanning measurements of nuclear fuel is displayed in figure 3.1, see e.g. chapter 4 and papers II and III.

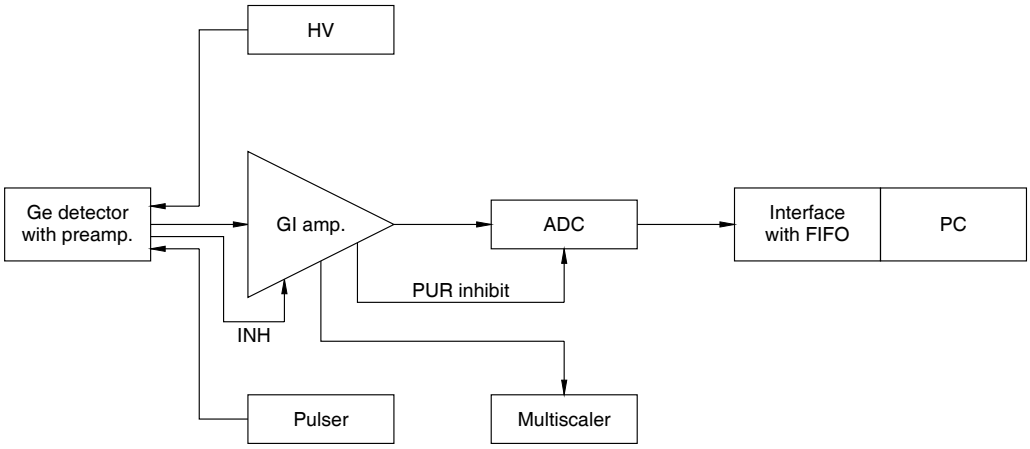

Figure 3.1: *Block scheme of the electronics used in gamma scanning. Abbreviations used here: HV = High voltage, GI = Gated integrator, INH = Inhibit, PUR = Pile-up rejection and FIFO = First in, first out circuitry.*

In the latter parts of the work, a PC-card[4] was utilized that contains all the essential NIM-electronics on a single card, i.e. amplification and multichannel analyzing capability. In the tomography application, see chapter 4,

[2]Model: ND 582 with a fixed conversion time of 1.5 μs.
[3]Model: GammaData PC16BIV2.
[4]Model: GammaFast 5004 from Aptec-NRC Inc.

this card was used. This commercially available card allows for count rates over 100 kcps with minimal spectrum distortion. Due to the PC-card format, which allows installation in a transportable computer, fuel measurements are more easily performed compared to bringing the NIM crate and associated electronics along for the experiment. Some features of the card used are listed below:

- Spectroscopy amplifiers with bipolar, unipolar, and gated integrator shaping type.
- Software driven peak digital stabilizer circuits.
- ADC and memory of 2, 4, 8, or 16k channels.
- Multiple time constants.
- ADC fixed conversion time of 800 ns including less than 200 ns to add one event into memory.
- Single plug-in card, industry standard 16 bit ISA full length slot, AT height, x86 or Pentium compatible.

3.1.3 Deadtime correction

The time period during which the detector system processes one event is called the deadtime. There are two general types of deadtime: 1) Extendable (also called paralyzable) deadtime where the deadtime is extended upon the arrival of a second pulse, i.e. the detector system is sensitive to pulses during deadtime. 2) Non-extendable (also called non-paralyzable) deadtime where the arrival of a second pulse simply is not detected, i.e. the system is insensitive to pulses during deadtime. In the first case, pile-up of events may distort the signal which can lead to loss of the information from both events. In the second case, events which arrive during dead time are lost. Thus, monitoring of the deadtime of the detector system is required in order to compensate for loss of events so that the true count rate is measured. For more details on deadtime and correction methods, see refs. [28, 29, 30].

The deadtime of a data acquisition system may be significant at high count rates. To accurately compensate the measured count rate for deadtime, one of several methods may be utilized, e.g. pulser-based correction, electronic correction or using a reference source (see below). In the gamma scanning application, the pulser-based deadtime correction method was used while in the tomographic application, the electronic correction method was used.

Reference source

By using a calibrated reference source in a fixed position relative to the detector, pulses are inserted into the data acquisition system. The reference source peak activity is known, which makes a dead time correction possible. The correction factor is simply the ratio of the rate of the reference source pulses and the rate of the reference source peak pulses as measured in the spectrum. In principle, this method is the most accurate method. However, a source with an appropriate gamma-ray energy or half-life may not always be available. Furthermore, the peak area of the reference source may not always be readily measured due to interference with other peaks in the gamma-ray energy spectrum.

The pulser method

The pulser method uses a pulse generator to generate an electric pulse which is led into the electronics system through the pre-amplifier circuit. Using a pulser frequency much lower than the spectrum count rate, one may assume that the artificial pulse is subject to the same deadtime as the gamma-ray pulses. The correction factor is calculated in a manner similar to the reference source method.

The assumption of equal deadtime of the pulse from the pulse generator and gamma-ray events may not always be valid. Pulses generated by commonly used pulse generators are, in general, not Poisson distributed. Furthermore, the peak shape of the artificial pulse may sometimes differ from the true events implying a risk of difference in deadtime due to varying processing in the amplifier electronics. Including these drawbacks, the uncertainty of the deadtime correction factor can, however, be as low as 0.1% [28]. The major advantages of this method are that the amplitude of the inserted pulse can be adjusted so that the artificial peak is positioned in the spectrum in order to avoid interference with the gamma-ray peaks of interest and that the width of the pulser peak can be relatively small, which implies high accuracy in determining the area of the pulser peak.

Electronic correction

The electronic correction operates using fast-timing electronics. The electronics start the deadtime when an event occurs with a fixed pileup rejection interval. When two or more pulses arrive within the interval, they are discarded and the count time is extended to compensate for the loss.

Another method of extending the count time is by starting the deadtime interval when a pileup event occurs and ending it when the next good event

occurs. The time between a pile-up event and the next good event is stored as an extended deadtime.

Even though this method is an approximation since it does not compensate for undetected events, but using a typical rejection-gate period of 20 μs and a pulse-pair resolving time of about 120 μs, the uncertainty of the correction may be only a few percent [28].

3.2 Neutron detector systems

Several types of neutron detectors are used for the study of nuclear material: Gas-filled detectors such as helium-, BF_3- or CH_4-filled detectors, fission chambers, and organic and inorganic scintillators. One common detector used by safeguard authorities is the FORK detector, see e.g. ref. [28], which is equipped with fission chambers. The FORK detector is shown in figure 3.2. The detection efficiency of fission chambers is relatively low, but since the detector is used in the unshielded flux density from a spent nuclear fuel assembly, an appropriate count rate is still achievable.

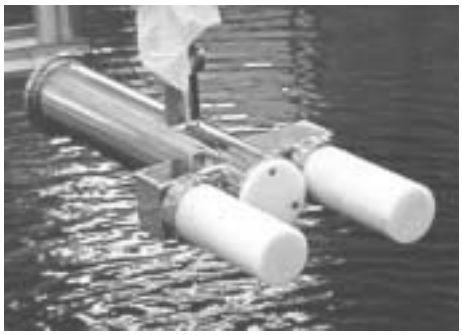

Figure 3.2: *The FORK detector. Picture from [31].*

Both active and passive measurements can be used for neutron assay. In active assay, an external source of neutrons is used to induce fission in the fuel under study and the emitted fission neutrons are measured. However, due to safety regulations, active neutron assay methods have not been pursued in this work. In passive assay, spontaneous fission neutrons emitted by the fuel are measured.

Chapter 4

Methods & applications

Basically, three methods for characterization of nuclear fuel assemblies by means of nuclear spectroscopy have been studied in this work:

1) Gamma-scanning

2) Gamma-ray tomography

3) Passive neutron measurements

4.1 Gamma scanning

Measurements of gamma radiation emanating from irradiated nuclear fuel has proven to be suitable for characterizing the reactor fuel after irradiation [32, 33]. In the case of gamma scanning, the fuel is scanned axially using a gamma detector in order to determine the axial intensity profile and/or the bundle average intensity of the radiation detected. A complex gamma-ray source such as nuclear fuel contains many decaying fission products which necessitates good energy resolution of the detector system used in order to resolve peaks in the gamma-ray energy spectrum. In this respect, germanium detectors are the obvious choice. However, for e.g. fuel with a long cooling time, where the gamma-ray spectrum is dominated by ^{137}Cs, measurements using detectors with less good energy resolution are often more economically attractive. For such cases, even gross gamma measurements using ion chambers may sometimes suffice. Figure 4.1 shows a typical setup where the whole length of a fuel assembly is scanned. For some purposes, scanning may also be performed on individual fuel rods [34].

Prior to measurements, the spent fuel assemblies are positioned into a fixture that can be elevated and rotated relative to a horizontal collimator mounted in the pool wall. Such equipment is available at the Swedish and

Finnish nuclear power plants and at CLAB. The fixture at CLAB comprises a motorized control of both the vertical and rotational motion of the fuel as indicated in figure 4.1. With the motor controls, the fuel bundle can be positioned within a few mm and one degree, respectively. The detector, in turn, is located downstream the collimator in a room which also contains the data acquisition system and arrangement for cooling of the detector.

The heart of the detector system is a large, typically 50 %-60 % Germanium detector. In this work, a N-type, coaxial Ge detector[1] with an energy resolution of 2 keV at 1332 keV gamma-ray energy was used. A sketch of the electronics used for the measurements in this setup is displayed in figure 3.1.

The iron collimator used is 1.2 m in length, 1-5 mm in height and with a width that varies from 8.2 cm at the detector end to 23.4 cm at the fuel end. Thus it is wide enough to cover the diagonal length of a PWR fuel assembly. The distance between the detector end of the collimator and the centre of the fuel is 2.46 m. With this collimator, the gamma-ray source seen by the detector is a slice of fuel with a height from 1.5 mm to 7.4 mm, depending on the height of the collimator slit used.

Using this equipment, the four corners of a fuel assembly are scanned axially at a speed of typically about 1.5 meters per minute. By scanning the corners of the assembly, the error in the measured intensity due to uncertainty in the rotational position is minimized. This is illustrated in figure 4.2, where the gradient of the intensity as a function of rotational angle is minimized at multiples of 90 degrees indicating a corner position. Usually, data from an axial scan is stored in about 200 spectra. The reproducibility of measurements of a certain full energy gamma-ray peak intensity, averaged over the fuel assembly (4×200 spectra), is about 0.5 %, ref. [35]. With this system the total measuring time for one assembly is typically about ten minutes.

[1]Manufactured by Eurisys Measures.

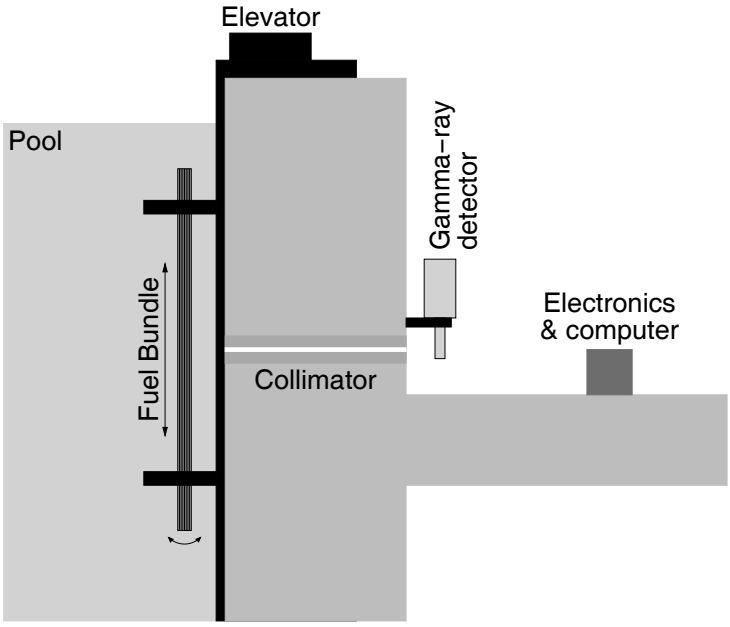

Figure 4.1: *Schematic view of a gamma scanning setup.*

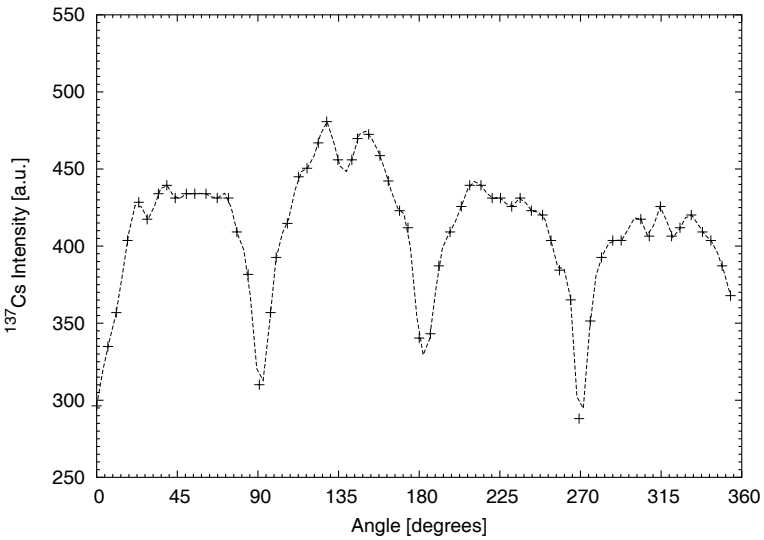

Figure 4.2: *Measured gamma-ray intensity from ^{137}Cs as a function of azimuthal angle of the fuel assembly in the gamma scanning equipment. Adapted from ref. [36].*

4.1.1 Verification of fuel parameters for safeguard purposes

Fuel parameters such as burnup and cooling time may be determined or verified using information obtained from measurements using the gamma scanning equipment. How this is pursued is the subject of this section.

Determination of burnup and cooling time

Isotopes of interest for measurements of gamma-rays from spent fuel are listed in table 2.3. For determination of burnup via equation 2.3, the following characteristics of the nuclide are of importance [32]:

- The nuclide should have a long half-life compared to the periods of irradiation.
- The fission yields of the nuclide from U and Pu should be approximately equal and well known, see equation 2.3.
- The nuclide should have low neutron-capture cross-sections like all precursors as well.
- The gamma-ray spectrum should be easily resolvable.
- The nuclide should have low migration in the fuel matrix. This also applies to the precursors.

To this list one may add that the energy of the gamma-ray measured should be as high as possible in order to facilitate the penetration of the fuel matrix.

Of the isotopes mentioned in table 2.3, the best burnup indicator is ^{137}Cs. It fulfils all criteria in the list above except the fifth item. The concentration of the isotope ^{137}Cs is very nearly proportional to the burnup of the nuclear fuel since it is produced as a direct fission product. Data from gamma-scanning measurements show that within 0.7% (1σ uncertainty of the linear slope coefficient), there is indeed a linear relationship between the burnup and measured gamma-ray intensity as shown in figure 4.4.

The relatively low gamma-ray energy of 662 keV (see figure 2.6 and table 2.3) implies that measurements of ^{137}Cs represent mainly the outer rows of rods in the fuel assembly, see figure 4.3. However, at the end of the irradiation, the burnup of the fuel assembly is generally relatively constant over the assembly cross-section, which makes measurements of peripheral values reasonably representative of the whole assembly.

A cross-section of an 8×8 BWR fuel assembly is shown in figure 4.3. The fuel pins made of UO_2 pellets enclosed in zircalloy cladding are strong attenuators of gamma-rays at the energies encountered in this work, see table 2.3.

The attenuation within a fuel assembly varies strongly, which implies a careful correction for self-attenuation of the gamma-rays for applications that are based on measurements of the spatial activity distribution. An example of such an application is tomography, described in section 4.2.

In the case of gamma scanning of fuel assemblies, the activity distribution may be assumed to be essentially homogeneous over the assembly, see above. In this case, correction for self-attenuation within the fuel may thus be omitted while still obtaining adequate accuracy.

Furthermore, attenuation of the gamma-rays within materials between the fuel and the detector must be taken into account when absolute measurements of the activity within the fuel are performed. In the case of gamma scanning, where relative measurements are performed with a permanent experimental geometry, such a correction is in general not needed. However, a small uncertainty in the intensity measurement due to uncertainty in positioning of the gamma scanning equipment relative the fuel assembly is introduced, see e.g. [36].

Migration of cesium to the periphery of the fuel rods has been reported by e.g. refs. [37, 38], which report migration to the edges of the fuel rods and that the effect is correlated with the temperature distribution within the fuel rod. The cesium tends to migrate against the temperature gradient and a higher temperature seems to increase the migration rate. In principle, migration may affect the measuring results. However, any effect from migration is expected to be well within the measuring accuracy and has not been a subject for closer investigation in this work.

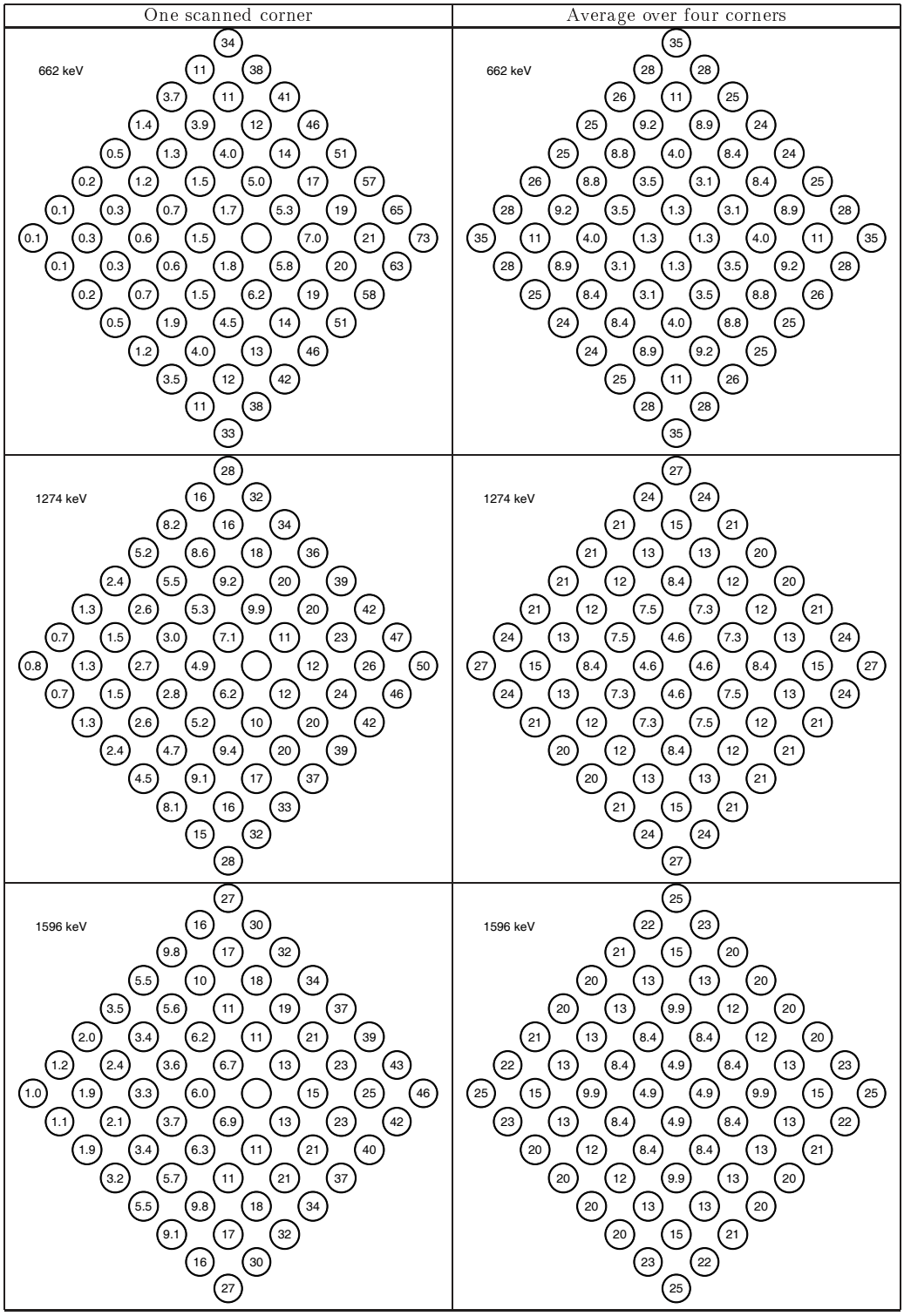

Figure 4.3: *Distribution of the contribution to the gamma-ray flux density of the full energy absorption peak at the detector position in figure 4.1 from a BWR 8x8 assembly for a few gamma-ray energies, calculated with MCNP [26]. The right corner of the assembly is facing the collimator and the detector. The contributions are shown in per mille of the total radiation emitted from the assembly. Some fluctuations occur due to statistics in the Monte Carlo calculation. The decrease in contribution seen in the upper right row of the left figures is caused by increasing attenuation of the gamma radiation in water.*

The production of the isotope ^{134}Cs is approximately proportional to the burnup to the power of two since it is mainly produced via neutron capture in the direct fission product ^{133}Cs. This process is dominated by resonance absorption, see figure 2.4. The burnup is thus roughly linearly correlated to the intensity-ratio ^{134}Cs/^{137}Cs, see e.g. [32]. However, since the half life of ^{134}Cs is only 2.1 years, the use of this ratio is limited to fuel assemblies with a relatively short cooling time. On the other hand, this ratio, as a measure of burnup, has the advantage that measurements using different detector setups may be directly compared since most factors of importance to the efficiency cancel out. A difference in migration rate between ^{137}Cs and ^{134}Cs has been observed, see e.g. refs. [32, 33]. The final distribution of ^{134}Cs is determined by the migration rate of its precursors ^{133}I and ^{133}Xe. The long half-lifes of its precursors, as compared to the precursors to ^{137}Cs, suggests that ^{134}Cs migrates more readily than ^{137}Cs.

The production path of ^{154}Eu is more complicated, as indicated in figure 2.5. Also, the ^{154}Eu fission yields for Uranium and Plutonium, respectively, are different, which complicates the relation between the burnup and the intensity of ^{154}Eu. Experimental data on measurements of the ^{154}Eu intensity show, however, that the production may approximately be represented as proportional to the burnup to the power of 1.5-2.0 [39], depending on irradiation history. The half life of ^{154}Eu is 8.6 years, implying that measurements up to about two decades after the end of irradiation of the fuel are possible.

The half lives of the isotopes ^{144}Pr and ^{106}Rh are too short to make them generally suitable as indicators of the burnup. Further, ^{106}Rh tends to migrate towards the centre of a rod [32, 37, 38]. They are, however, both produced from beta decay of precursors produced directly by fission and they may therefore be suitable to use as indicators of burnup at relatively short cooling times. Also, ^{144}Pr has a distinct advantage because of it's high gamma-ray energy of 2.2 MeV, implying a high penetrability through the fuel assembly.

Figure 4.4 shows experimental data on the correlation between declared burnup and measured gamma-ray intensities from ^{134}Cs, ^{137}Cs and ^{154}Eu. The relation between the measured gamma-ray intensity I and burnup may generally be written as equation 4.1:

$$I = k\beta^{\kappa} \cdot e^{-\lambda T} \tag{4.1}$$

Even though this equation, except for ^{137}Cs, is an approximation to a complicated production mechanism (and other forms for expressing the relation between gamma-ray intensity and burnup may be established), it is empirically a relatively good approximation as shown in figure 4.4. A strong covariance exist between the fitted parameters k and κ for ^{134}Cs and ^{154}Eu,

which must be taken into account when evaluating measurements.

Figure 4.4 illustrates how the burnup of an assembly may be determined. The functions drawn in figure 4.4 have been fitted to equation 4.1 with the parameters shown in table 4.1. Using a specific data-set as a calibration and fitting the curve given by equation 4.1 to that data, the burnup β_i of another assembly i of the same type may thus be determined with the same measuring setup using equation 4.2:

$$\beta_i = \sqrt[\kappa]{\frac{I_i}{k}\exp(\lambda T_i)} \tag{4.2}$$

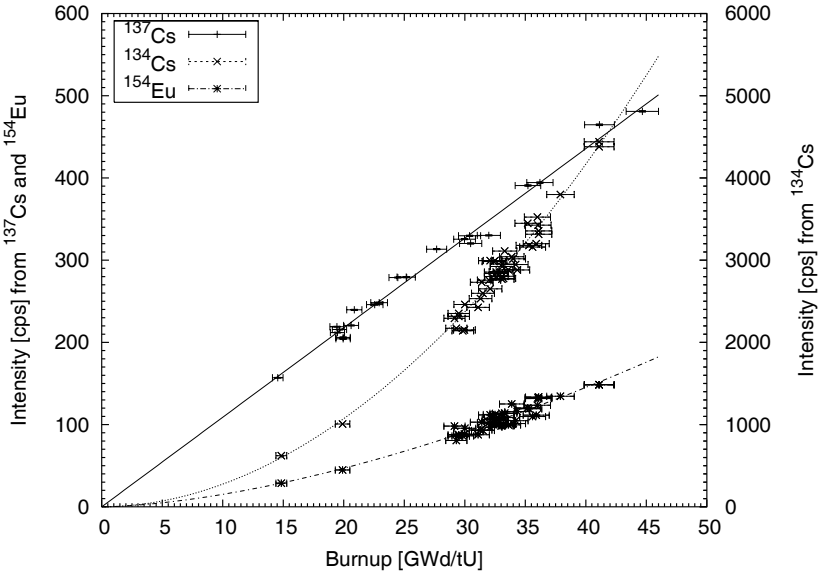

Figure 4.4: *Experimental data on the correlation between burnup and the gamma-ray intensity from various isotopes. The gamma-ray intensities were adjusted to correspond to the intensities at the end of irradiation. The lines are fitted to the history (α) corrected intensity data, a line was fitted to the ^{137}Cs and power functions were fitted to the ^{134}Cs and ^{154}Eu data. Parameters of the fitted functions are shown in table 4.1. Data on ^{137}Cs is from [40], data on ^{134}Cs and ^{137}Eu are from [41].*

The calibration constant k depends on the experimental geometry (including the fuel assembly geometry) and detection efficiency of the detector system. One may factorize the calibration constant according to $k = k' \cdot T \cdot \Omega \cdot \epsilon$, where the factors in order are first the source strength per burnup unit (i.e. gamma-ray activity per burnup), the average transmission of radiation from

Parameter	^{137}Cs	^{134}Cs	^{154}Eu
k	10.89(8)	3.0(8)	0.4(2)
κ	*1*	1.96(7)	1.6(1)

Table 4.1: *Parameters of equation 4.1 fitted to the experimental data on the correlation between burnup and the gamma-ray intensity from various isotopes shown in figure 4.4. The equation fitted to the history (α) corrected intensity data. For ^{137}Cs, the parameter κ was fixed at one. The gamma-ray intensities were adjusted to correspond to the intensities at the end of irradiation.*

the source to the detector, the solid angle between the detector and source and last, the intrinsic detection efficiency of the detector.

The intensity I is determined in a relative measurement. Therefore, data-sets from measurements using different setups need to be normalized if they are to be compared. This may be performed in various ways: 1) Measuring the same fuel assembly in the two setups. 2) A transportable gamma-ray source may be used [36]. 3) For ^{137}Cs, a linear fit of the declared burnup vs. measured gamma-ray intensities (I_1, corrected for decay time to the end of the last fuel cycle) $I_1 = k_1 \cdot \beta$ can be performed for setup 1. The ratio (k_1/k_2), obtained from two setups 1 and 2, may used as normalization constant.

Application of equation 4.1 above requires knowledge of the cooling time T of the assemblies. This information should normally be available from the operators, but one may foresee cases when this information is uncertain or even unavailable when the burnup is to be determined. Combining measurements of two isotopes, one may form a system of equations like equation 4.1, which, when solved, yields the expression given in equation 4.3, which is independent of the cooling time. Here, the exponentials $\kappa_{i=1,2}$ must be such that $\lambda_2\kappa_1 \neq \lambda_1\kappa_2$.

$$\beta = \exp\left[\frac{\ln\left\{\left(\frac{k_2}{I_2}\right)^{\lambda_1} \cdot \left(\frac{I_1}{k_1}\right)^{\lambda_2}\right\}}{\lambda_2\kappa_1 - \lambda_1\kappa_2}\right] \tag{4.3}$$

Measurements on two different isotopes can also be used to determine the cooling time independently of burnup. Solving a system of equations like 4.1 for the cooling time, using measurement data on two isotopes, yields the expression in equation 4.4. As in equation 4.3, the exponentials $\kappa_{i=1,2}$ must be such that $\lambda_2\kappa_1 \neq \lambda_1\kappa_2$.

$$T = \frac{\ln\left\{\left(\frac{k_2}{I_2}\right)^{\kappa_1} \cdot \left(\frac{I_1}{k_1}\right)^{\kappa_2}\right\}}{\lambda_2\kappa_1 - \lambda_1\kappa_2} \tag{4.4}$$

Correction for irradiation history

Basically, the activity of a fission product depends, besides on burn-up and cooling time, also on the number and length of the power cycles, i.e. the irradiation history. To be able to compare measurements on fuel assemblies with different irradiation histories, the measured gamma-ray intensities should be corrected accordingly. First, the measured gamma-ray intensity is corrected for the decay to an appropriate time reference, usually to the end of irradiation, i.e. corrected for the cooling time. Second, a correction factor is introduced [41] that takes into account the irradiation history, i.e. the dates of irradiation and the burn-up contribution per irradiation cycle, as declared by the operator.

Assuming that an isotope with half life λ is produced linearly with the constant reactor power p, during cycle n of length τ_n, for instance ^{137}Cs, the amount N_n of that isotope is governed by the differential equation 4.5. The solution in equation 4.6 describes the build-up of the isotope during irradiation. The first term describes the production, with k being a proportional constant, while the second term represents the decay, with decay constant λ.

$$\frac{dN_n}{dt} = kp - \lambda N_n \tag{4.5}$$

$$N_n(\tau_n) = \frac{kp}{\lambda}\left(1 - e^{-\lambda\tau_n}\right) \tag{4.6}$$

Figure 4.5 shows the build-up of such an isotope during a sequence of irradiation cycles. In ref. [41], a correction factor α is introduced as the ratio between a hypothetical case when the decay of the isotope is ignored and the real case in which the decay during irradiation and between cycles is included. Referring to figure 4.5, the correction factor α is the ratio between the two quantities N_0 and n_0 as given in equation 4.7.

$$\alpha = \frac{N_0}{n_0} \tag{4.7}$$

or,

$$\alpha = \frac{\sum\limits_n \beta_n}{\sum\limits_n \frac{\beta_n}{\lambda\tau_n}\left(1 - e^{-\lambda\tau_n}\right)e^{-\lambda t_n}} \tag{4.8}$$

Here, t_n is the length in time between the end of irradiation cycle n to the end of the last irradiation cycle and β_n is the burnup aquired during cycle n. Table 4.2 shows typical values of α.

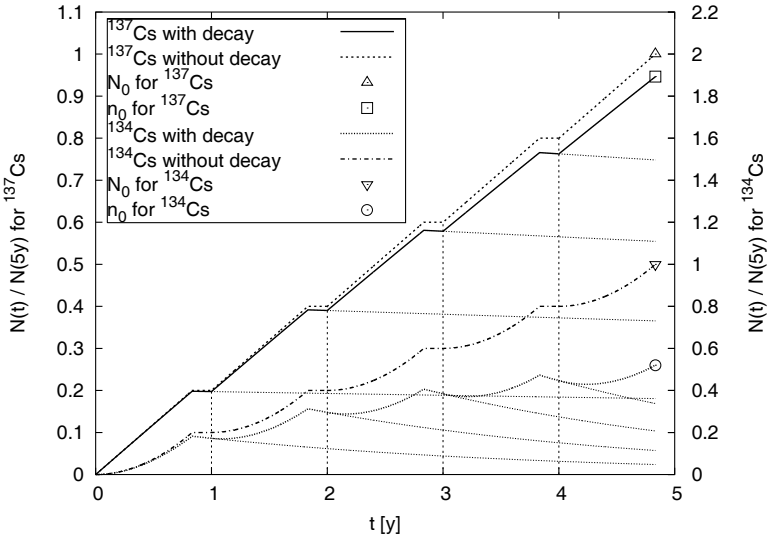

Figure 4.5: *The buildup of ^{134}Cs and ^{137}Cs. Two curves shown for each isotope: One when the decay during irradiation is taken into account and one when it is not. In this case, data for ^{134}Cs and ^{137}Cs was used. Five irradiation cycles with constant power during ten months of irradiation per cycle with two months shutdown period is assumed. The curves have been normalized to the content at t=5y for the case without decay.*

Assuming that an isotope is produced non-linearily with power, e.g. ^{134}Cs or ^{154}Eu, according to the expression $N_n = k'\beta_n^\kappa$, then equation 4.5 is generalized to the expression given in equation 4.9, see ref. [39]. The solution to equation 4.9 is given in equation 4.10, which in general can not be calculated analytically and must therefore be approximated.

$$\frac{dN_n}{dt} = \kappa k' p^\kappa t^{\kappa-1} - \lambda N_n \tag{4.9}$$

$$N_n(\tau_n) = \kappa k' p^\kappa e^{-\lambda\tau_n} \int_0^{\tau_n} t^{\kappa-1} e^{\lambda t} dt \tag{4.10}$$

Writing the expression for the correction factor α in this case yields equation 4.11, where t in the integral has been substituted by $x \cdot \tau_n$, and $(p\tau_n)^\kappa = \beta_n^\kappa$. Equation 4.11 reduces to 4.8 when $\kappa = 1$. Table 4.2 shows typical values of α including both the linear and the non-linear case. As seen in table 4.2, α depends strongly on the half-life of the isotope and the irradiation history for all isotopes except ^{137}Cs.

$$\alpha = \frac{\sum_n \beta_n^\kappa}{\sum_n \kappa\beta_n^\kappa e^{-\lambda(\tau_n+t_n)} \int_0^1 x^{\kappa-1} e^{\lambda x\tau_n} dx} \tag{4.11}$$

Introducing the correction factor α into equations 4.1, 4.3 and 4.4 yields the expressions in equations 4.12 and 4.13 for determining the burnup and cooling time, respectively.

$$\beta = \exp\left\{\frac{\ln\left[\left(\frac{k_2}{\alpha_2 I_2}\right)^{\lambda_1} \cdot \left(\frac{\alpha_1 I_1}{k_1}\right)^{\lambda_2}\right]}{\lambda_2\kappa_1 - \lambda_1\kappa_2}\right\} \tag{4.12}$$

$$T = \frac{\ln\left\{\left(\frac{k_2}{\alpha_2 I_2}\right)^{\kappa_1} \cdot \left(\frac{\alpha_1 I_1}{k_1}\right)^{\kappa_2}\right\}}{\lambda_2\kappa_1 - \lambda_1\kappa_2} \tag{4.13}$$

Even though equations 4.12 and 4.13 are explicitly independent on the cooling time and burnup, respectively, the calculation of $\alpha_{i=1,2}$ does, however, require information on the irradiation history of the assembly. The irradiation history may thus be verified to some extent by the results of the gamma scanning. The examples given in table 4.2 illustrate how the history correction factor depends strongly on the irradiation history, especially for the short-lived isotopes. Since the declared irradiation history is used to calculate α, falsified records of irradiation dates will result in a correction factor that puts the data point of the assembly off the average trend.

Isotope	κ	Number of cycles					$\langle\Delta\alpha/\alpha\rangle$
		3	4	5	6	7	[%]
^{137}Cs	1.0	1.032	1.044	1.056	1.068	1.080	1.1
^{134}Cs	2.0	1.464	1.678	1.905	2.145	2.397	12
^{154}Eu	1.6	1.107	1.150	1.194	1.240	1.286	3.7
^{144}Pr	1.0	2.597	3.322	4.078	4.858	5.650	19

Table 4.2: *Values of the history correction factor α calculated for some isotopes for different power histories. Each cycle was assumed to be 10 months of irradiation and 2 months of shutdown. The burnup acquired per cycle was assumed constant (β_n in equation 4.11 was constant). The last column shows the average relative increase in α per cycle, in percent.*

4.1.2 Decay heat in spent fuel

In Sweden, the spent nuclear fuel is planned to be encapsulated in copper and steel canisters and deposited within the bedrock at a depth of about 500 meters, see section 1.2. The surface temperature of the canister has to be limited to 100 °C [11] and the maximum total decay heat of the fuel assemblies placed within the canister is therefore, according to ref. [42], limited to 1800 W. On the other hand, in order to minimize the costly need for storage of the spent fuel before encapsulation and to minimize the amount of canisters needed, the decay heat of the assemblies put in the canisters should be as close to the design limit as possible. Therefore, an accurate knowledge of the decay heat of each fuel assembly is needed prior to encapsulation.

After 40 years of cooling, the typical decay heat of a spent fuel assembly is in the order of 100 W and 500 W for BWR and PWR fuels, respectively. There may, however, be substantial fluctuations between fuel assemblies depending on their burnup and other fuel parameters. It is anticipated that the encapsulation procedure can not rely entirely on decay heat calculations, since they are based on the assumption that the operators data are available and indisputable. Also, the uncertainties associated with the calculations may in some circumstances be unacceptably high. Therefore, measurements of the decay heat is the preferred choice.

An existing method to measure the decay heat using calorimetry is too time consuming as it takes in the order of 24 hours to determine the decay heat for one assembly. Therefore, a new method to determine the decay heat of spent nuclear fuel experimentally has been developed and evaluated.

The method is based on gamma-ray measurements where it takes about 10 minutes to determine the decay heat. This is about a factor of 100 faster than with a calorimetric method, implying that the decay heat can be determined on a routine basis when handling the spent fuel, for instance in the encapsulation plant of a final repository. Therefore, the experimental method described here offers an attractive alternative to theoretical calculations.

When the fuel has been stored for about 40 years, the significant gamma radiating isotope is ^{137}Ba, following β^- decay of ^{137}Cs. As seen in table 2.2, about 35%, of the total heat generated in spent nuclear fuel arises from the decay of ^{137}Cs. Using the ORIGEN code, we have shown that the relative contribution to the heat from the decay of ^{137}Cs, for the fuel parameters of interest during encapsulation, is constant within a few percent with respect to variations in the fuel parameters, see figure 4.6 and table 2.2. Therefore, it should be possible to determine the decay heat experimentally from gamma-ray measurements of ^{137}Cs.

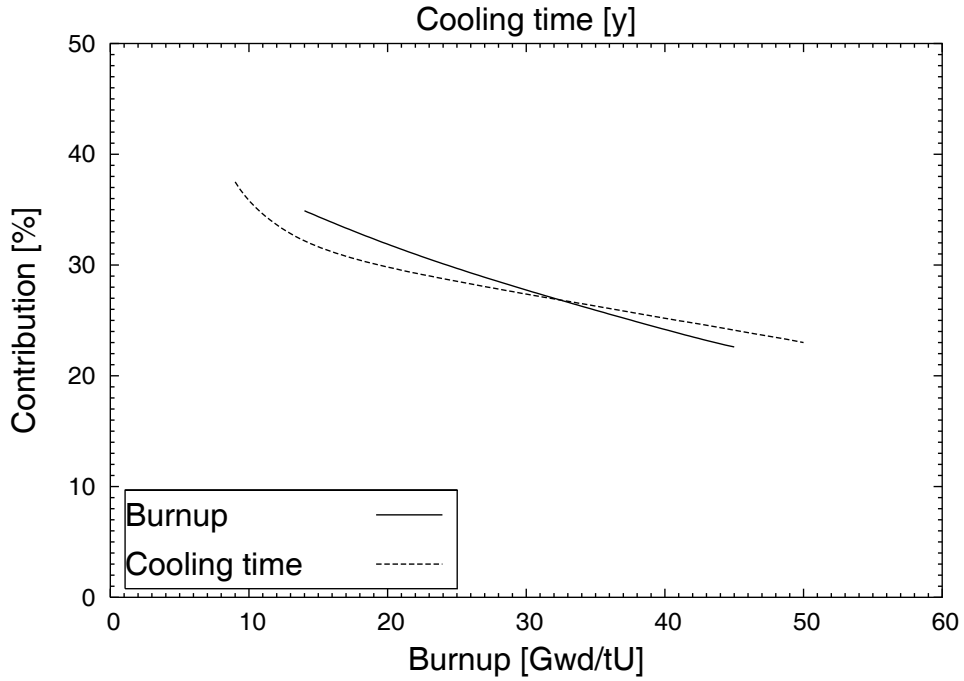

Figure 4.6: *The contribution to the decay heat from decay of ^{137}Cs as a function of burnup and cooling time, adapted from [40].*

The heat produced in the decay of ^{137}Cs is directly proportional to the activity (A) of ^{137}Cs in the fuel: $P_{137} = k \cdot A$. P_{137} may be written as $f \cdot P$ where f is the fraction of the total decay heat (P) originating from the decay of ^{137}Cs. Thus, $P = k \cdot A/f$. Further, assuming a homogenous activity distribution, implying a proportionality between the total ^{137}Cs activity and the measured ^{137}Cs gamma intensity, the total decay heat can be expressed as:

$$P = C \cdot \frac{I}{f} \tag{4.14}$$

Where,

- P is the residual thermal power of the fuel assembly.
- C is a calibration constant expressed in W/counts/s. This constant depends on the measuring geometry, fuel type and intrinsic detector parameters and C includes the ratio between measured ^{137}Cs intensity and the activity of ^{137}Cs.
- I is the measured count rate of ^{137}Cs.

To first order, the fraction f can be considered to be constant ≈ 0.25 for a typical fuel assembly, see figure 4.6. For an accuracy better than 10%, the constant has to be slightly corrected for variations in burnup and cooling time. The factor f is determined by using the ORIGEN code for a set of assemblies with different burnup and cooling time. Using the computer results, a linear function of burnup and cooling time is used to interpolate the f-factor for a particular fuel assembly.

In normal reactor operation, the fraction f is relatively insensitive to variations in fuel parameters as outlined above. There are cases however, when the relative contribution to the total decay heat from ^{137}Cs varies more strongly. For cooling times shorter than ≈ 10 years, f varies non-linearily with cooling time, see figure 4.6, due to the contribution of short-lived isotopes which are produced in a complicated process. For initial enrichments in the range than 1-4 percent, f varies with about 2 percent units per unit change in enrichment, see paper III.

A project was initiated in order to experimentally investigate the potential of using high-resolution gamma-ray spectroscopy to determine the decay heat. A number of fuel elements were measured with regard to the decay heat and with regard to the emitted gamma radiation. The first parameter was determined using a calorimetric technique. The calorimeter equipment and measurements are described in refs. [43, 44, 45]. Essentially, the calorimeter consists of a steel box submerged in water, enclosing the spent fuel assembly. The fuel assembly heats the water inside the calorimeter and the temperature difference between the interior and the exterior of the box is measured when thermal equilibrium is reached. This tempererature difference is a function of the heat generated by the spent fuel. Using an electrically heated model of the spent fuel, a calibration curve was established between (electrical) power and the temperature difference.

For the gamma-ray measurements, the gamma scanning equipment discussed in section 4.1 was used to measure the average intensity of ^{137}Cs from the assemblies. In this context it may be noted that in addition to decay heat, parameters relevant for safeguard can be determined simultaneously. Paper III and references [46, 47, 40] gives a detailed report of the achievements in the project. It was shown that the decay heat can be determined with a relative uncertainty of about 3% for BWR and PWR spent fuel assemblies.

4.2 Tomography

There are circumstances when measurements are required on individual fuel rods rather than complete fuel assemblies. For instance, the smallest entity treated in reactor core calculations of e.g. the thermal power distribution

was, for a long time, a slice of the nuclear fuel assembly. The increase of the computer capacity during later years has made possible the development of codes which comprise more detailed models of the fuel.

To experimentally validate such core simulators it is necessary to measure separate fuel rods. Earlier, measurements have been carried out by removing single rods out of a fuel assembly [34]. However, such measurements are expensive to carry out extensively and also involve non-negligible risks, especially after short cooling times. An alternative way is apply tomography in order to obtain information without the need of dismantling the fuel assemblies. Such an approach would also give much more data since all fuel rods in an assembly are taken into account.

Another potential field of application of the tomographic technique is the verification of the integrity of nuclear fuel assemblies. Verifying the fissile content of spent fuel against operator declared data is an important task in IAEA safeguards. Spent fuel is stored for relatively long times before encapsulation and several scenarios of a wrongly declared fissile content are possible, e.g. fuel rods may have been replaced during operation or rods may have been removed for other reasons i.e. for using the fissile material in undeclared activities. Once the spent fuel has been encapsulated for e.g. a deep geological storage, it will be very difficult to access. Therefore verification of partial defects immediately before encapsulation is anticipated to be performed by safeguard inspection.

An important part of the work was to investigate the potential of a tomographic method and eventually build a test equipment for tomographic measurements on fuel assemblies. The technique investigated utilizes single photon emission tomography to extract the spatial activity distribution within a fuel assembly from the measured gamma-ray intensity distribution around the assembly. The principle of emission tomography on a nuclear fuel assembly is shown in figure 4.7.

4.2.1 Reconstruction method used

In tomography it is a common practice to divide the object under study into imaginary, geometrical subparts, e.g. two-dimensional picture elements (pixels). In the case of studies of nuclear fuel assemblies, the two-dimensional division is justified because we measure the radiation from a small "slice" of the fuel height over which the variation of the gamma-activity along the height of the assembly is negligible.

During the reconstruction, the pixels are assigned the proper activity values in order to account for the measured intensity distribution. Generally in tomography, the pixels are evenly distributed because the geometry of an

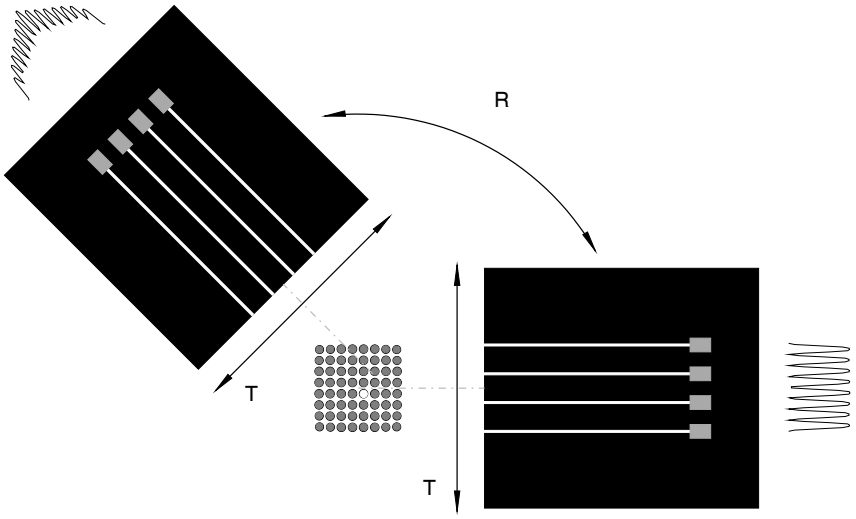

Figure 4.7: *The principle for emission tomography on a BWR 8×8 nuclear fuel assembly. R=Rotation and T=Translation. The black rectangles are collimators with four detectors. The intensity patterns obtained by translating the collimators are indicated.*

object is not known. However, if the geometry is known, as is the case for fuel assemblies, a fast and accurate technique is to locate the pixels at radiating positions, i.e. at the position of the fuel rods. This is the basic principle for the reconstruction technique developed in this work for studies of nuclear fuel and it is illustrated by equation 4.15.

In equation 4.15, the activity distribution $\mathbf{A}$ in N pixels is reconstructed from the measured intensity distribution $\mathbf{I}$ outside the assembly (measured in M positions). $\mathbf{W}$ is a matrix describing the transport of the gamma radiation from the point of emission in the assembly to the detector. The reconstruction is performed by solving equation 4.15 for $\mathbf{A}$.

In principle, $\mathbf{W}$ can be calculated to arbitrary precision using the knowledge of geometrical properties and material constants of the source-detector system. In practise, however, the calculation of $\mathbf{W}$ is time consuming even for a fast computer. In our case, we approximate the matrix $\mathbf{W}$ by using a point kernel method to calculate w_{ij}.

More detailed information on the basic principles used can be found in ref. [48].

$$\begin{pmatrix} w_{11} & w_{12} & \cdots & w_{1N} \\ w_{21} & w_{22} & \cdots & w_{2N} \\ \vdots & \vdots & \ddots & \vdots \\ w_{M1} & w_{M2} & \cdots & w_{MN} \end{pmatrix} \cdot \begin{pmatrix} a_1 \\ a_2 \\ \vdots \\ a_N \end{pmatrix} = \begin{pmatrix} i_1 \\ i_2 \\ \vdots \\ i_M \end{pmatrix} \qquad (M > N) \tag{4.15}$$

4.2.2 Verification of fuel for safeguard purposes

Paper II describes the techniques and results obtained in a measurement performed on a spent fuel assembly in CLAB. The experiment was performed on a complete BWR 8×8 assembly, which had an empty water channel in the central part of the assembly. To test the tomographic technique we assumed a complete fuel assembly, i.e. even the water channel contained fuel. With such an assumption, the calculation of **W** is wrong for those pixels that correspond to the water channel and we can thus test the ability of the technique to reveal a missing pin at that location. Measurements of the ^{137}Cs peak at 662 keV and of the ^{154}Eu peak at 1274 keV were performed using the gamma scanning equipment at CLAB, described in section 4.1. The setup was modified by rotating the collimator slit 90 degrees into a vertical position and aligning it in parallell with the symmetry axis of the fuel assembly. The width of the collimator slit was 1 mm. The vector **I** of equation 4.15 consisted of the intensities of the full energy absorption peaks in 2520 positions relative to the fuel. The results from the tomographic reconstruction significantly revealed an empty position in the central part of the assembly. The reconstructed activity in the empty position was about 60% of the average activity, i.e. about 4σ smaller than the average.

Even though the equipment used for this experiment was not originally designed for a tomographic measurement, the results indicate that the tomographic technique has a potential as a valuable tool for verification of integrity.

4.2.3 Code validation - PLUTO

It is known [32], that the activity of ^{140}La is a good measure of the power outtake just before shutdown. Therefore, measurements of the thermal power in fuel rods have been performed by dismantling fuel assemblies and by measuring the activity of ^{140}La in individual rods [34].

Preferably, the relative uncertainty of the measured activity distribution within a fuel assembly should be in the order of or less than the uncertainty associated with the computer calculations. The uncertainty of the results from modern nodal codes are expected to be in the order of a few percent

[49]. Therefore, a tomographic device has been constructed for tomographic measurements where the goal has been to reach a relative uncertainty of 1%.

To meet the demand of 1% uncertainty, special considerations were taken into account when constructing the tomographic device. Thorough simulations were performed, ref. [50], in order to define the mechanical constraints governing the design. A conceptual design according to figure 4.8 was developed. The following characteristics can be noted:

- Dimensions and handling routines are the same as for the transport cask used for transporting Swedish irradiated fuel to the interim storage.
- Ballast is applied to the device for stability.
- During measurement, the device is placed at the bottom of a fuel handling pool.
- Two radii of the axial-through channel are allowed for, in order to be adapted for BWR and PWR fuel, respectively.
- Fuel assemblies are transported into the equipment with normal equipment and routines.
- The fuel assembly to be measured is placed in an axial-through channel, allowing for cooling by a free flow of pool water.
- The fuel stays put during measurement, i.e. no fuel handling is performed by the measuring device.
- During measurement, the elevator table is positioned at desired axial position. Here, the angular rotations in steps of 5-10 degrees are performed. At each angular position, measurements are performed at different lateral positions in steps of 1-2 mm.

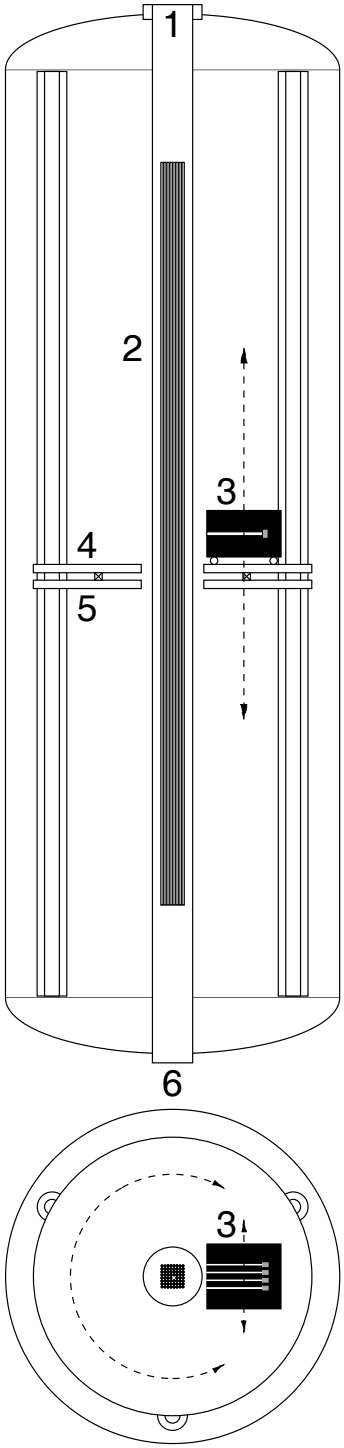

Figure 4.8: *Schematic construction of the tomographic equipment. The total height and diameter of the eqipment is 5.1 and 1.8 meter, respectively. 1) Axial-through channel (waterfilled). 2) Fuel assembly. 3) Collimator and detector system. 4) Rotation table. 5) Elevator table. 6) Water inlet.*

The device is controlled from an industrial PC, which allows all motion and data collection to be controlled by software. The software supplies a user interface in the form of a panel from which commands can be executed. A complete tomographic measurement can be performed automatically by executing a prepared command sequence. The software includes in the order of 100 subroutines. The status of all subsystems is controlled repeatedly during execution. An overview of how the hardware and software functions in the device interact is shown in figure 4.9.

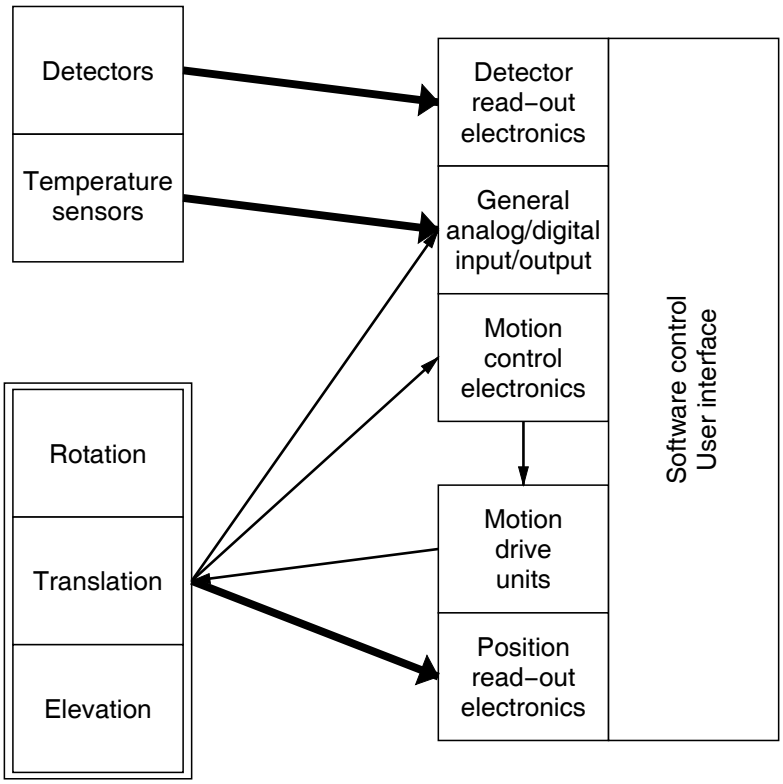

Figure 4.9: *Block diagram showing the most important interaction between hardware and software in the tomographic device. Items on the left hand side are situated in the measuring device. Thick arrows indicate data that are logged for off-line analysis capability.*

Ge-detectors were considered too expensive and complicated as radiation detectors for the present application, a more adequate solution was found by using BGO scintillation detectors. Their relatively low energy resolution can be accepted because the 1596 keV peak from ^{140}Ba/La is the dominant peak in the gamma-ray energy spectrum around 15 days of cooling time. The peak is also relatively well isolated in the spectrum. The temperature coefficient of the ouput of BGO is relatively large, which implies that temper-

ature measurements are desirable for monitoring the thermal stability, and the system must allow for repeated controls of the detector efficiency. It is estimated that a BGO detector system can measure a count rate in the order of 10^5 cps without loss of efficiency or resolution, implying that a system with in the order of 5-10 parallel detectors is required to perform a tomographic measurement on 25 axial nodes in eight hours.

The equipment was demonstrated in paper IV to operate well in a test measurement on fuel with a cooling time of 8 months. A few improvements are being implemented before the first test on freshly irradiated fuel. It is expected that the equipment, in addition to verification of computer codes, could be used to study the consequences on the thermal power distribution caused by mechanical distortions like e.g. box bending in BWR fuel.

4.3 Neutron measurements for safeguard verification

The spent nuclear fuel contains isotopes that fission spontaneously under neutron emission, mainly ^{242}Cm and ^{244}Cm, see table 2.4. In principle, this neutron signal from the fuel can be used in order to determine the amount of fuel present. This is the basis for the work performed by IAEA inspectors when implementing safeguards using the FORK detector, [51], see figure 3.2.

It has been suggested in e.g. ref. [36] that by measuring the neutron flux density and the gamma-ray flux density from e.g. ^{137}Cs simultaneously one may get a rough indication on the completeness of the fuel assembly, i.e. if there are fuel pins missing. This is a simple and fast measurement as opposed to the tomography method described in section 4.2.2.

To investigate the potential of this method, a simulation study of the neutron- and gamma-ray fields outside irradiated BWR 8×8 fuel assemblies was performed, in which fuel rods were assumed to be removed or replaced by lead rod dummys. Specifically, two effects were studied: (i) To what extent the radiation fields are influenced by the number of replaced rods and (ii) to what extent the radiation field for a specific number of replaced rods depends on the geometric pattern of the replaced rods.

Calculations of the effect of missing and/or replaced rods in a BWR 8×8 spent fuel assembly were performed using ORIGEN-S [19] and the Monte Carlo code MCNP-4C [26]. To some extent, the results of the calculations could be validated with experiments performed at the Swedish interim storage CLAB, where measurements with a FORK detector were performed, see e.g. refs. [52, 53].

The computer simulations showed that the ratio between the average

thermal neutron flux density and the gross gamma-ray flux density from the assembly depends linearly on the amount of missing fissile mass, see figure 4.10. When the rods are replaced with e.g. lead rods, however, the gamma-ray signal is strongly dependent on the pattern of the replaced rods (due to the relatively strong attenuation of the gamma-rays in the lead as compared to in water) and yields no correlation to the missing fissile mass. In that case, the neutron flux density alone is a better signal of the fissile mass content since the neutrons are relative insensitive to the lead. The results suggest that 3 % of the fuel mass may be significantly (4σ) detected as replaced, i.e. 2 out of 63 rods, independently of the pattern of replaced rods, from measurements of the average thermal neutron flux density. More details on the calculations may be found in paper V.

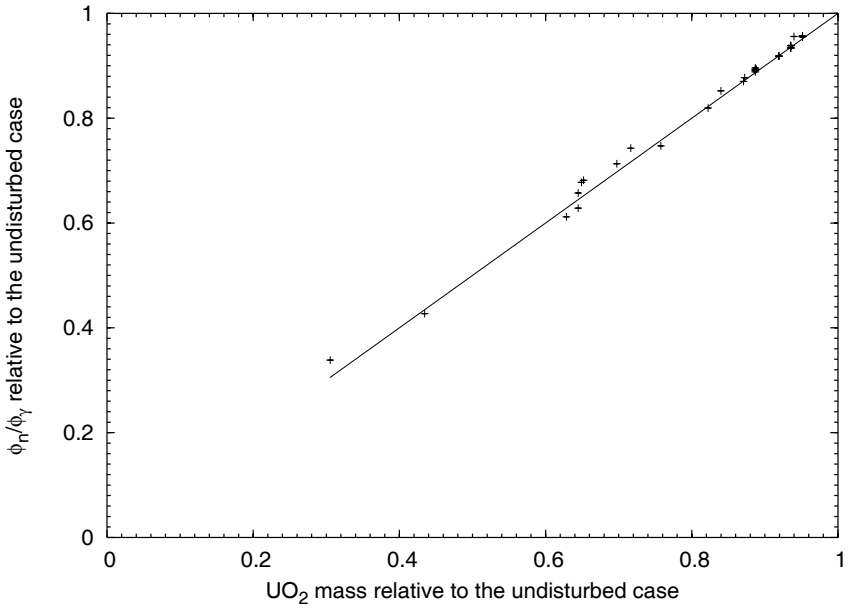

Figure 4.10: *The ratio of the gross neutron flux and the gross gamma-flux vs. the fuel mass, relative to the undisturbed case. The line is a guide for the eye.*

Chapter 5

Conclusions and outlook

To summarize this thesis, studies of nuclear fuel by means of nuclear spectroscopy methods have been shown to be valuable tools for characterization of nuclear fuel.

For the immediate future, a further development of the projects initiated during this work is envisioned. Calorimetric measurements of the decay heat in spent fuel assemblies before encapsulation are planned to be made on a regular basis combined with the gamma-ray spectroscopy method described. The tomographic apparatus built is planned to be used by the nuclear power industry in Sweden and Finland for measurements of the power profile just before the end of the irradiation periods. Besides its immediate purpose to verify core simulators, one may foresee studies of thermal power deviations caused by mechanical distortions such as e.g. box bending.

Measurement methods described in this work, may also be put in a general, long term perspective. With the terrorist attacks on September 11, 2001, in the USA, an increase in IAEA activities to strengthen non-proliferation surveillance techniques is foreseen, ref. [54]. This implies that measurement techniques such as those presented in this thesis, will be of increased importance for safeguards in the future.

In view of the intensive discussions going on regarding the effect of increasing emission of greenhouse gases worldwide, one may think of a renaissance of nuclear power. Firstly, there is an obvious need to replace old reactors in a relatively near future with energy production systems that minimizes the emission of greenhouse gases. Secondly, states that today almost entirely rely on fossil fuels are under pressure to change their energy policy owing to the Kyoto protocol. Especially one would think of countries in the third world that are likely to meet a much more energy consuming future and are presently extensive users of fossil fuel.

In this perspective it may be a possible scenario that the world community may have to re-evaluate nuclear power and seriously discuss the initiation of

a new nuclear-power program that comprises a major part of the world. That such a scenario would demand a strong and complete safeguards system is evident.

New reactor concepts may also be an important part of the above scenario and here one can anticipate extensive research in order to develop experimental techniques for various characterization tasks. The methods presented in this thesis may well serve as starting points for new methods and techniques.

Chapter 6

Summary of papers

This thesis is based on the following papers, which are referred to in the text by their Roman numerals:

Paper I

I. Matsson, P. Jansson, B. Grapengiesser, A. Håkansson and A. Bäcklin. (1998). Fission Gas Release Determination Using an Anti-Compton Shield Detector. Nuclear Technology, NUTYBB **122** (3) 276-283 (1998), ISSN 0029-5450. (Manuscript.)

Abstract

Poolside measurements of fission gas release (FGR) in fuel pins have been made using gamma-ray spectroscopy with a Ge detector, measuring ^{85}Kr activity in the fuel rod plenum. The gamma-ray energy spectra from irradiated nuclear fuel are characterized by prominent Compton distributions that can obscure the weak 514-keV ^{85}Kr peak. To improve the sensitivity, the detector has been provided with an anti-Compton shield of six $Bi_3Ge_4O_{12}$ detectors[1]. Laboratory tests of the detector system showed that the maximum peak-to-Compton (p/c) ratio was improved by a factor of ∼6. The results of the poolside measurement p/c ratio showed a somewhat smaller improvement (a factor of ∼4) because of scattered gamma radiation from the surrounding material. However, the precision in the poolside FGR measurements was improved substantially utilizing the Compton shield.

[1]Authors note: The abstract published for paper I contains a small type error, the correct formula for BGO is $Bi_4Ge_3O_{12}$ according to ref. [55].

Paper II

S. Jacobsson, A. Håkansson, P. Jansson and A. Bäcklin. A Tomographic Method for Verification of the Integrity of Spent Nuclear Fuel Assemblies - II: Experimental Investigation. (2001). Nuclear Technology, NUTYBB **135** (2) 146-153 (2001), ISSN 0029-5450. (Manuscript.)

Abstract

A tomographic method for verification of the integrity of used light water reactor fuel has been experimentally investigated. The method utilizes emitted gamma rays from fission products in the fuel rods. The radiation field is recorded in a large number of positions relative to the assembly, whereby the source distribution is reconstructed using a special-purpose reconstruction code.

An 8×8 boiling water reactor fuel assembly has been measured at the Swedish interim storage CLAB, using installed gamma-scanning equipment modified for the purpose of tomography. The equipment allows the mapping of the radiation field around a fuel assembly with the aid of a germanium detector fitted with a collimator with a vertical slit. Two gamma-ray energies were recorded, 662 keV (^{137}Cs) and 1274 keV (^{154}Eu). The intensities measured in 2520 detector positions were used as input for the tomographic reconstruction code. The results agreed very well with simulations and significantly revealed a position containing a water channel in the central part of the assembly.

Paper III

P. Jansson, A. Håkansson, A. Bäcklin and S. Jacobsson. (2002). Gamma-ray Spectroscopy Measurements of Decay Heat in Spent Nuclear Fuel. Nuclear Science and Engineering 141 1-11 (2002). (Accepted.)

Abstract

A method for determining the residual thermal power in spent nuclear fuel using gamma-ray spectroscopy is suggested. It is based on the correlation between the residual power and the ^{137}Cs activity, which is nearly linear for fuel with cooling times between 10 and 50 years. Using available data of calorimetrically measured values of the decay heat in 69 boiling water reactor and pressurized water reactor spent fuel assemblies resulted in an agreement with a standard deviation of 3%.

Paper IV

P. Jansson, S. Jacobsson, A. Håkansson and A. Bäcklin. (2002). PLUTO - A Device for Non-destructive Experimental Determination of the Power Distribution in Nuclear Fuel Assemblies . Nuclear Science and Engineering. (To be published.)

Abstract

A device for experimental determination of the thermal power distribution in the fuel rods in BWR and PWR fuel assemblies is described. It is based on measurements of the 1.6 MeV gamma radiation from decay of ^{140}Ba/La and utilises a tomographic method to reconstruct the pin-by-pin source distribution. No dismantling of the fuel asembly is required.

The device is designed to measure an axial node in 20 minutes with a precision better than 2% (1σ). It is primarily planned to be used for verification of core calculation codes and for studies of deviations in thermal power caused by mechanical distortions such as box bending.

Paper V

P. Jansson, A. Håkansson and A. Bäcklin. (2002) Neutronic effects of partial defects in BWR 8×8 spent fuel assemblies . Nuclear Technology. (Submitted.)

Abstract

The possibility of detecting replaced fuel rods in a spent fuel assembly by means of measurement of the emitted neutron and gamma-ray radiation has been investigated by computer simulations. The radiation field outside a BWR 8×8 fuel assembly with varying patterns of fuel rods replaced with lead dummys was modeled using a simple model for the source distribution and the Monte Carlo code MCNP-4C for the radiation field. Also, calculations of the gamma and neutron response of a modified FORK detector were performed for four assemblies for comparison with experiments performed at CLAB.

The results suggest that 3 % of the fuel mass may be significantly (4σ) detected as replaced, i.e. 2 out of 63 rods, independently of the pattern of replaced rods, from measurements of the average thermal neutron flux density.

Chapter 7

Acknowledgments

There are very many people that deserve credit for helping me to this point. Of course, someone may be forgotten in this relatively short acknowledgment. The possibility of corrupted memory bytes is certainly not intentional. Therefore, a distributed thanks to all those forgotten is hereby executed.

First and foremost, I would like to thank my supervisors Prof. Anders Bäcklin and Dr. Ane Håkansson for their wisdom, strong support and valuable discussions during my time as a PhD student. Anders, thank you especially for questioning me, back in 1995, about interest in that diploma work, which subsequently led me to my current position. If it were not for that particular moment, the risk that I would have gone elsewhere would have been quite high. Ane, thank you especially for guiding me into the world of gamma-rays and computer programming in those early days of scanning nuclear fuel in campaign L. If it were not for that early experience with the people and atmosphere in the business, I might have been doing something rather different.

A student in nuclear physics is sometimes working late and sleeping too little. Therefore, a vacation in the middle of everything is appreciated. A big thanks goes to my colleague Staffan Jacobsson for all your (special) humor and also your suggestions and comments regarding our work during all these years. Our vacations in San Francisco, Oregon and Grand Canyon after the IRRMA'99 and WM'01 conferences will be remembered with warmth.

All the other PhD students at the department of radiation sciences and the neighboring department of neutron research, should also receive thanks for establishing the nice environment in which we work. The coffee breaks we share are a constant source of happiness. I would like to extend gratitude to all those of you who have been my coffee colleagues these years. Special thoughts and ideas are sometimes developed during relaxing conditions where they can be discussed freely. Therefore, special thanks goes to Anders Hjalmarsson, Cecilia Johansson, Christofer Willman, Hans Henriksson and

Joakim Klug for all those nice discussions we had during relaxing conditions. I hope they will continue.

Special considerations should also be given to other supporting people. Especially, I would like to thank the administrative personnel, Inger Ericson and Eva Forsman, for their great efforts with providing solutions to all kinds of problems. Also, Ib Koersner and Roger Ruber deserve credit for their work with the computer systems and for surviving my torturing of all those central processing units.

Speaking of thanks, distribution of thanks and cpu's, I would like to take the opportunity here to distribute something back (in the form of a thank you) to all the people behind the $\sim 3 \cdot 10^4$ anonymous cpu's that generously contributed computing power to my distributed calculations.

Last, but not least, thoughts should be given to my family. Mother, thank you for always giving me support, strength and nourishment. Annika, thank you for being my sister and for bearing with me and my habits. Sonny, thank you for our nice moments with good food, good company and nice little projects around the house. Carina, thank you too for supporting me in these final moments of my PhD studies.

References

[1] Suresh Garg, Ferosh Ahmed, and L.S. Kothari. *Physics of nuclear reactors.* Tata McGraw-Hill Publishing Comp. Ltd., 1986.

[2] IAEA Power Reactor Information System database (PRIS), 2000. Available on-line: `http://www.iaea.org/programmes/a2/`.

[3] Kenneth S. Krane. *Introductory uclear physics.* John Wiley and Sons, Inc., 1988.

[4] T. R. England and B. F. Rider. Evaluation and Compilation of Fission Product Yields. Report LA-UR-94-3106, Los Alamos National Laboratory, October 1994.

[5] Data from the Isotopes Project at the NuclearScience Division at Lawrence Berkeley National Laboratory. Available on-line: `http://ie.lbl.gov/ip.html`.

[6] T-2 Nuclear Information Service at Los Alamos National Laboratory, 2002. Available on-line: `http://t2.lanl.gov/`.

[7] The Nuclear Fuel Cycle, February 2001. Appendix to Vattenfall Generation's certified envorinmental product declaration of electricity from Forsmarks Kraftgrupp AB, Sweden.

[8] Data from ENSDF as reported by Lund Nuclear Data WWW Service available on-line: `http://nucleardata.nuclear.lu.se/nucleardata/`.

[9] Westinghouse corporate information avaiable on-line: `http://www.westinghouse.com/`.

[10] The Virtual Nuclear Tourist available on-line: `http://www.nucleartourist.com/`.

[11] Deep repository for spent nuclear fuel, SR 97 - Post-closure safety. Technical Report TR-99-06, Swedish Nuclear Fuel and Waste Management Co (SKB AB), November 1999.

[12] Nuclear Energy Agency (NEA). Nuclear Energy in a Sustainable Development Perspective. Technical report, 2001. Report from NEA to the OECD Project on Sustainable Development.

[13] A. Tobias. Decay Heat. *Progress in Nuclear Energy*, 5(1):1–193, 1980.

[14] B Duchemin and C. Nordborg. DECAY HEAT CALCULATION An International Nuclear Code Comparison. Reports NEACRP-319-L and NEANDC-275-U, CEN Saclay and NEA Data Bank, France, 1988.

[15] Oak Ridge National Laboratory. *SCALE - A Modular Code System for Performing Standardized Computer Analyses for Licensing Evaluation*, 1997. NUREG/CR-0200, Rev. 5 (ORNL/NUREG/CSD-2/R5).

[16] O. W. Hermann and M. D. DeHart. Validation of Scale (SAS2H) Isotopic Predictions for BWR Spent Fuel. Report ORNL/TM-13315, Oak Ridge National Laboratory, Computational physics and eng. div., 1998.

[17] J. C. Ryman et al. Fuel Inventory and Afterheat Power Studies of Uranium-Fueled Pressurized Water Reactor Fuel Assemblies Using the SAS2 and ORIGEN-S modules of Scale with an ENDF/B-V Updated Cross Section Library. Report NUREG/CR-2397, ORNL/CSD-90, Union Carbide Corp., Nucl. Div., 1982.

[18] M.J. Bell. ORIGEN - The ORNL Isotope Generation and depletion code. Report ORNL-4628, Oak Ridge National Laboratory and Union Carbide Corp., Nucl. Div., May 1973.

[19] O. W. Hermann and R. M. Westfall. *ORIGEN-S: SCALE system module to calculate fuel depletion, actinide transmutation, fission product buildup and decay, and associated radiation source terms.* Oak Ridge National Laboratory, 1998. ORNL/NUREG/CSD-2/V2/R6, NUREG/CR-0200.

[20] The uranium institute, 1992.

[21] IAEA SAFEGUARDS CRITERIA, November 1990. Annex D, item 2, note (2).

[22] F.W. Walker, J.R. Parrington, and F. Feiner. Chart of the nuclides. Knolls atomic power laboratory, 14:th edition, april 1998.

[23] M.J. Berger, J.H. Hubbell, S.M. Seltzer, J.S. Coursey, and D.S. Zucker. XCOM: Photon Cross Section Database (version 1.2), 1999. Available: `http://physics.nist.gov/xcom` [2002, February 20].

[24] Data from ENDF-VI.7, retreaved from NEA data bank available on-line: `http://www.nea.fr/`.

[25] Data from JENDL-3.2, retreaved from NEA data bank available on-line: `http://www.nea.fr/`.

[26] J. F. Briesmeister. MCNP - A General Monte Carlo N-Particle Transport Code - Version 4C. Report LA-13709-M, Los Alamos National Laboratory, April 2000.

[27] A. Bäcklin, A. Håkansson, P. Björkholm, A. Dyring, and K-G. Görsten. A Gamma-Spectroscopy System for Burnup Measurements of Nuclear Fuel. May 1991. 13th ESARDA Symposium on Safeguards and Nuclear Material Management, Avignon, France.

[28] D. Reilly, N. Ensslin, H. Smith Jr., and S Kreiner. Passive Nondestructive Assay of Nuclear Materials. Reports NUREG/CR-5550 and LA-UR-90-732, US Nuclear Regulatory Commission and Los Alamos National Laboratory, March 1991.

[29] W. R. Leo. *Techniques for Nuclear and Particle Physics Eexperiments.* Springer-Verlag, 2:nd edition, 1994.

[30] Glenn F. Knoll. *Radiation detection and measurement.* Number ISBN 0-471-81504-7. John Wiley and Sons, Inc., 2:nd edition, 1989.

[31] Personal communications with J. Saarinen, VTT Energy Comp. Finland.

[32] S.T. Hsue, T.W. Crane, W.L. Talbert Jr., and John C. Lee. Nondestructive Assay Methods for Irradiated Nuclear Fuels. Report LA-6923 (ISPO-9), Los Alamos National Laboratory, January 1978.

[33] J.R. Phillips, J.K Halbig, D.M Lee, S.E. Beach, T.R Bement, E. Dermendjiev, C.R. Hatcher, K. Kaieda, and E.G. Medina. Application of Nondestructive Gamma-Ray and Neutron Techniques for the Safeguarding of Irradiated Fuel Materials. Report LA-8212 (ISPO-77), Los Alamos National Laboratory, May 1980.

[34] B. Grapengiesser and I. Matsson. Measurements on Fuel Assemblies from Leibstadt for Determination of Relative Power Distribution. Report BUC 97-048, ABB Atom AB, Sweden, August 1996.

[35] P. Björkholm and A. Dyring. A Study of a High Count Rate Gamma Spectrometer System for Burnup Measurements. Master's thesis, University of Uppsala, Institute of Technology, 1990. UPTEC 90015E.

[36] M. Tarvainen, A. Bäcklin, and A. Håkansson. Calibration of the TVO spent BWR reference fuel assembly. Report STUK-YTO-TR 37, Finnish Centre for Radiation and Nuclear Safety (STUK), 1992.

[37] R.S. Forsyth, W.H Blackadder, and N. Ronqvist. Burn-Up Determination by High-Resolution Gamma Spectrometry Fission Product Migration Studies. Report AE-272, Aktiebolaget Atomenergi AB, April 1967.

[38] J.R. Phillips. New Techniques in Precision Gamma Scanning, Application to Fast-Breeder Reactor Fuel Pins. Report LA-5260-T, Los Alamos Scientific Laboratory, July 1973.

[39] A. Håkansson. To be published.

[40] P. Jansson, A. Håkansson, S. Jacobsson, and A. Bäcklin. A Method of Meausuring Decay Heat in Spent Nuclear Fuel using Gamma-ray Spectroscoopy. In *Waste Management Symposium 2001*, February 2001.

[41] A. Håkansson and A. Bäcklin. Non-Destructive assay of spent BWR fuel with high-resolution gamma-ray spectroscopy. Report TSL/ISV-95-0121, ISSN 0284-2769, University of Uppsala, Dept. of Radiation Sciences, 1995.

[42] M. Wikström and A. Nyström. Private communications, 1999. Swedish Nuclear Fuel and Waste Management Company (SKB).

[43] L. Agrenius. Residual heat measurements in 14 BWR assemblies. Project memo 96-3430-07-CLAB, Swedish Nuclear Fuel and Waste Management Co (SKB AB), 1996.

[44] F. Sturek. CLAB - utvärdering av kalibreringskurva för kalorimetrisk mätning. Rapport, OKG AB, 1999.

[45] F. Sturek. CLAB - kalorimetrisk mätning av resteffekt på BWR-bränsle. Rapport, OKG AB, 1999.

[46] P. Jansson. Determination of the Residual Thermal Power in Spent Nuclear Fuel from Gamma-Ray Measurements. Report ISV-4/1997, University of Uppsala, Dept. of Radiation Sciences, 1997.

[47] P. Jansson, A. Håkansson, and A. Bäcklin. Gamma-Ray Measurements of Spent PWR Fuel and Determination of Residual Power. Report ISV-7/1997, University of Uppsala, Dept. of Radiation Sciences, October 1997.

[48] S. Jacobsson, C. Andersson, A. Håkansson, and A. Bäcklin. A tomographic method for verification of the integrity of spent nuclear fuel assemblies - I: Simulation studies. *Nuclear Technology*, 135(2):131–145, August 2001.

[49] Benchmark calculations of power distribution within fuel assemblies. Report NEA/NSC/DOC(2000)3, NEA Data Bank, France, 2000.

[50] S. Jacobsson, P. Jansson, A. Håkansson, and A. Bäcklin. A non-destructive tomographic method for experimental determination of the pin power distribution in nuclear fuel assemblies. To be published.

[51] IAEA. Safeguards techniques and equipment. International nuclear verification series, No. 1, 1997.

[52] A. Tiitta, J. Saarinen, M. Tarvainen, P. Jansson, A. Håkansson, and K. Jansson. Enhanced FORK Detector for Partial Defect Verification of BWR Fuel Assemblies. In *Proceesings, Symposium On International Safeguards, Vienna, Austria*. IAEA, 29 October - 1 November 2001.

[53] A. Tiitta and J. Hautamäki. Spent VVER fuel characterisation combining a FORK detector with gamma spectrometry. Report STUK-YTO-TR 181, Finnish Centre for Radiation and Nuclear Safety (STUK), August 2001.

[54] *IAEA Symposium on international safeguards, verification and nuclear material security*, 29 October– 2 November 2001. Special session, closing remarks by C. Curtis.

[55] R.K. Bock and A. Vasilescu. *The Particle Detector BriefBook*. Springer-Verlag Heidelberg, 1998. ISBN 3-540-64120-3.